Department of Information Optics, Faculty of Physics

University of Warsaw

Light transformations in metallo-dielectric nanolayers

NUSOD'08, Numerical Simulation of Optoelectronic Devices
1-5 September 2008, Nottingham, UK

Rafał Kotyński

1D Metallo-Dielectric Multilayers

Single Ag or LHM layer (Veselago, Pendry)

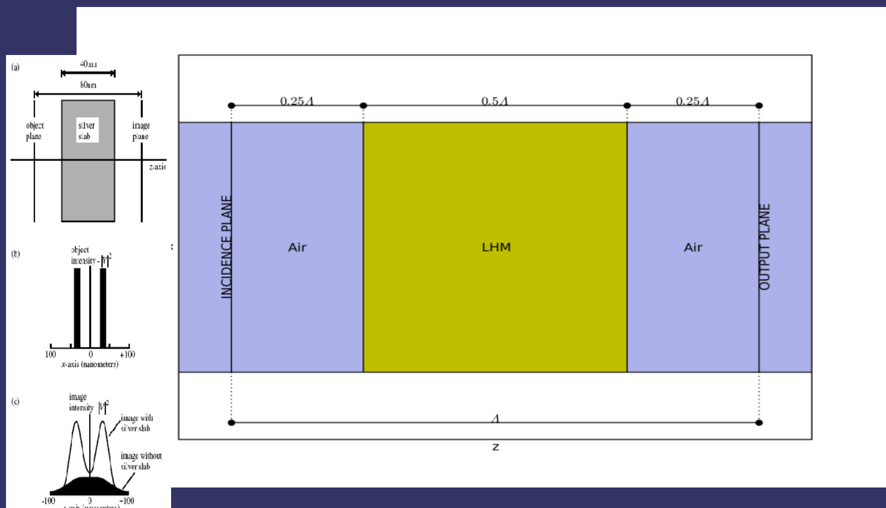

Resonant tunnelling (Scalora, Sibilia, ...)

Canalization (Belov, ...)

Layered lens (Pendry, ...)

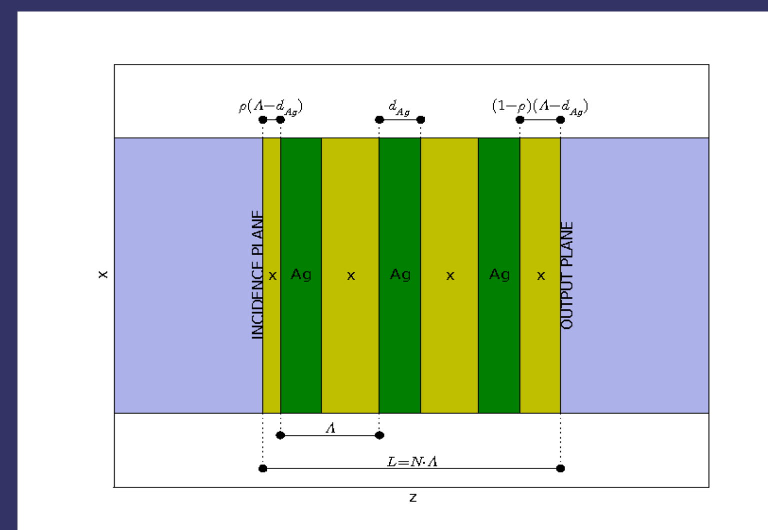

Asymmetric lens (Ramakrishna, Pendry, Schurig, Smith, Schultz, Fang, Zhang...)

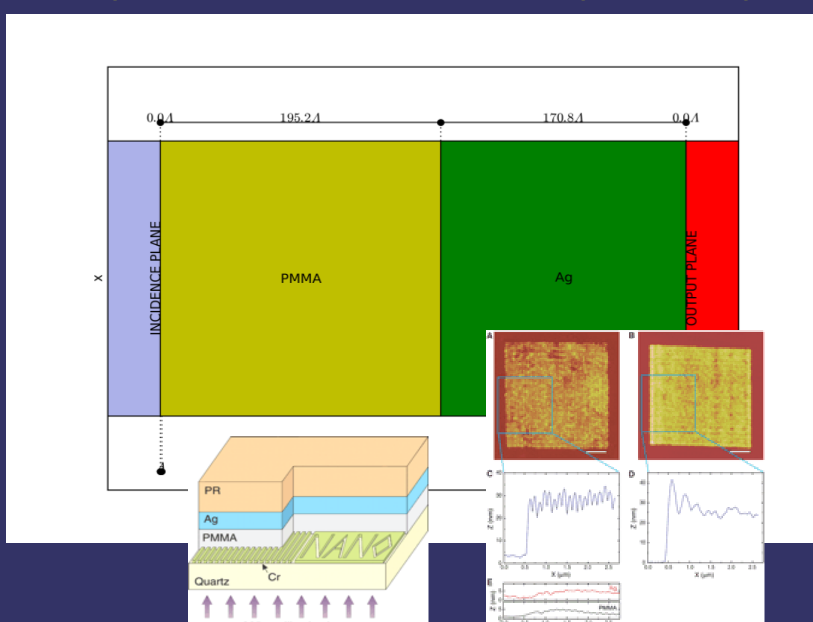

Linear Shift Invariant Systems (LSI)

INPUT PLANE

$E(x)$

Linear shift-invariant system

OUTPUT PLANE

$E'(x)$

SPATIAL DOMAIN:

$$E'(x) = H(x) * E(x)$$

PSF -Point Spread Function

convolution

FT

IFT

SPATIAL FREQUENCY DOMAIN:

$$\hat{E}'(k_x) = \hat{H}(k_x) \cdot \hat{E}(k_x)$$

MTF - Modulation Transfer Function

multiplication

Applications of spatial filtering

Fourier optics

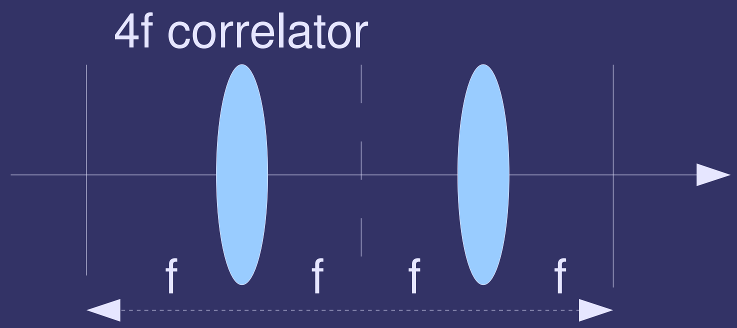

Fourier plasmonics (?)

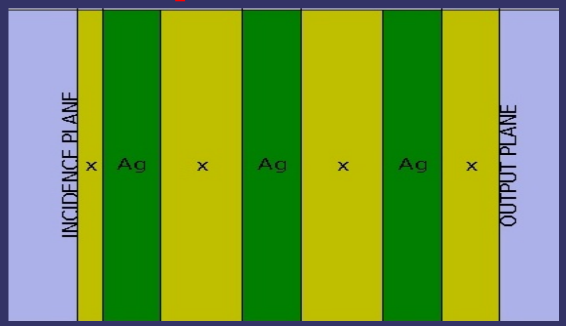

Macro-scale → Nano-scale

✓ **1. Imaging (superresolution)** ✓ superlens

$$\hat{H}_{norm} = \exp(-k_x^2/2\sigma_k^2) \quad \text{small } \sigma_k$$

✓ **2. Laplace filtering (edge detection)** ?

$$\hat{H}_{\delta^2} = -\alpha k_x^2$$

✓ **3. Beam splitting** ?

$$\hat{H}_{spl} = \cos(k_0 x_0)$$

✓ **4. Wiener filtering (noise removal)** ?

$$\hat{H}_{Wiener} = (1 + |\hat{f}|^2/|\hat{n}|^2)^{-1}$$

✓ **5. Matched filtering (pattern recognition)** ?

$$\hat{H}_{CMF} = \hat{f}^*$$

MTF – infinite uniform medium

$$\hat{H}_z(k_x) = \exp\left(i z \sqrt{n^2 k_0^2 - k_x^2}\right)$$

Propagation distance / wavelength

Dielectric (glass, n=1.5)

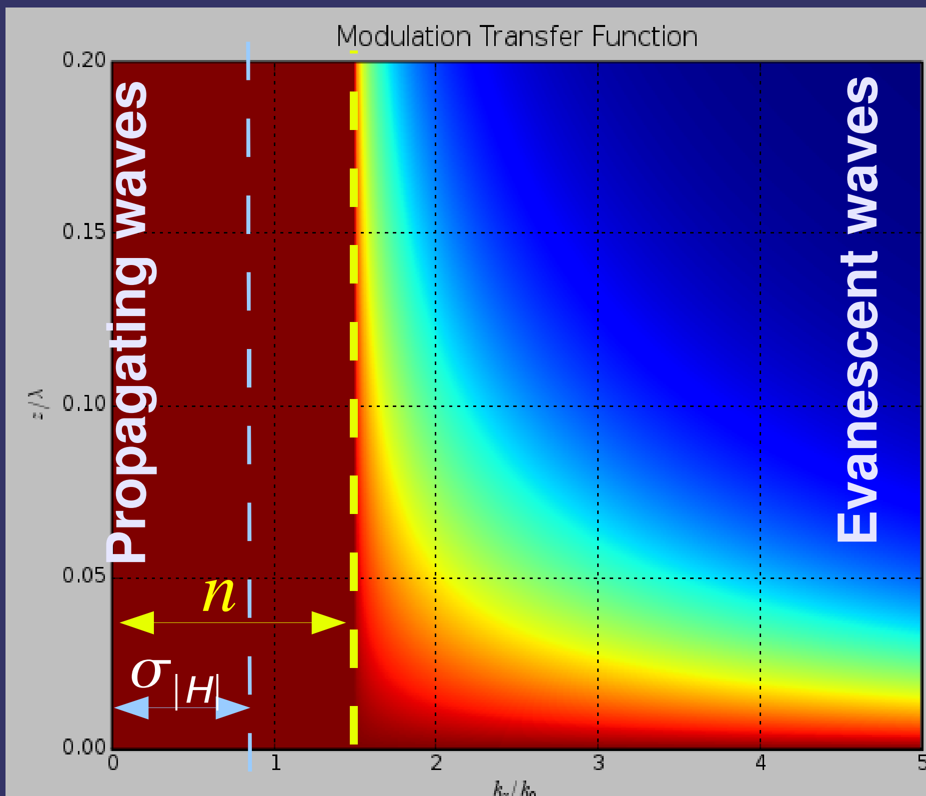

k_x / k_0

Metal (Ag at 500nm)

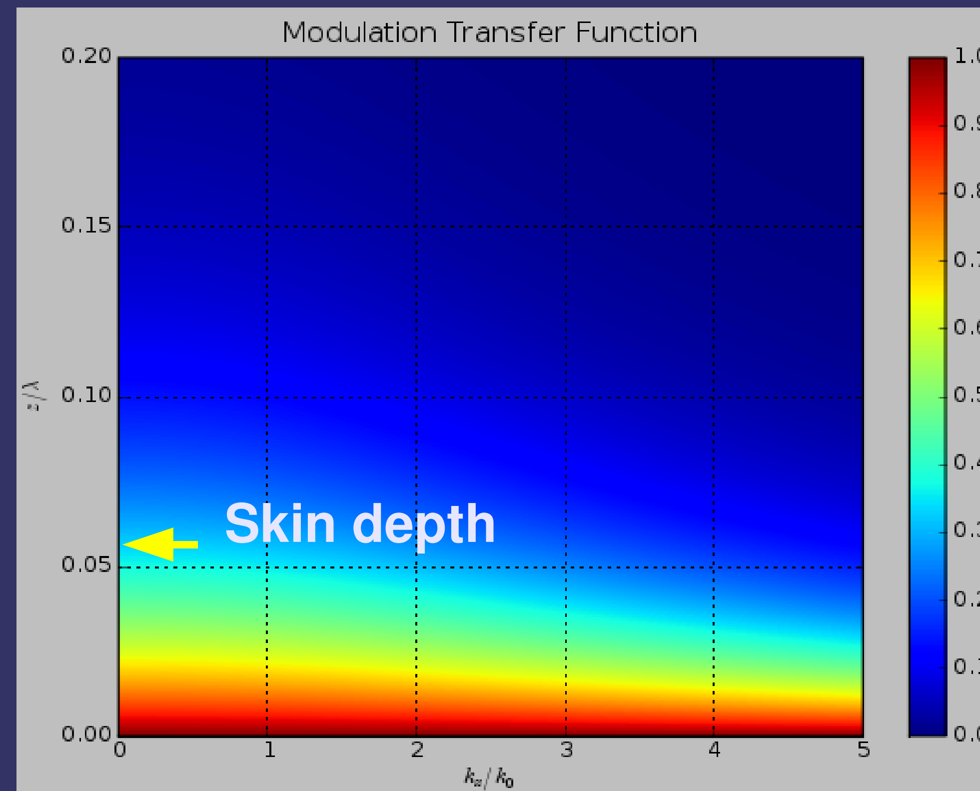

k_x / k_0

Uncertainty relation (1D): $\sigma_{|H|^2} \cdot \sigma_{|\hat{H}|^2} \geq \frac{1}{2}$

↓

Diffraction limit: $2.36\,\sigma_H \geq 0.5\,\frac{\lambda}{n}$

Layered structures

Transfer Matrix Method

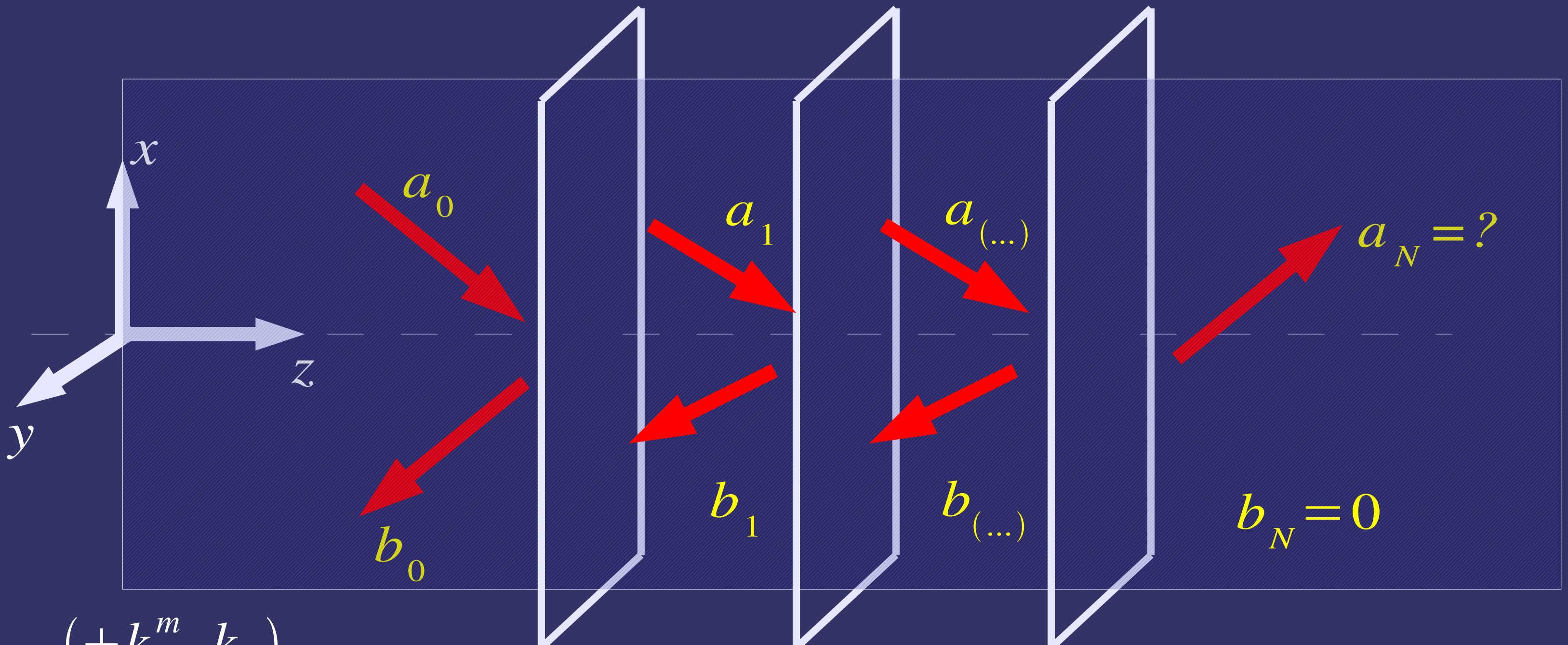

$(+k_z^m, k_x)$ $\quad a_m$ $\qquad\qquad a_{m+1}$ $\quad (+k_z^{m+1}, k_x)$

$$\begin{bmatrix} a_m \\ b_m \end{bmatrix} = \boldsymbol{T}^{m+1} \cdot \begin{bmatrix} a_{m+1} \\ b_{m+1} \end{bmatrix}$$

$(-k_z^m, k_x)$ $\quad b_m$ $\qquad\qquad b_{m+1}$ $\quad (-k_z^{m+1}, k_x)$

Transfer Matrix Method: $$\begin{bmatrix} a_0 \\ b_0 \end{bmatrix} = \overbrace{\boldsymbol{T}^1 \cdot \ldots \boldsymbol{T}^{N-1} \cdot \boldsymbol{T}^N}^{\boldsymbol{T}} \cdot \begin{bmatrix} a_N \\ b_N \end{bmatrix}$$

TMM – plane wave transmission

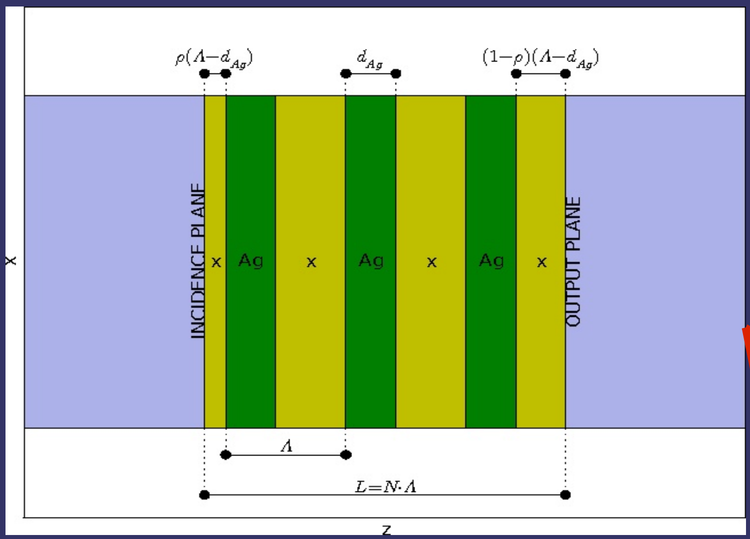

TMM

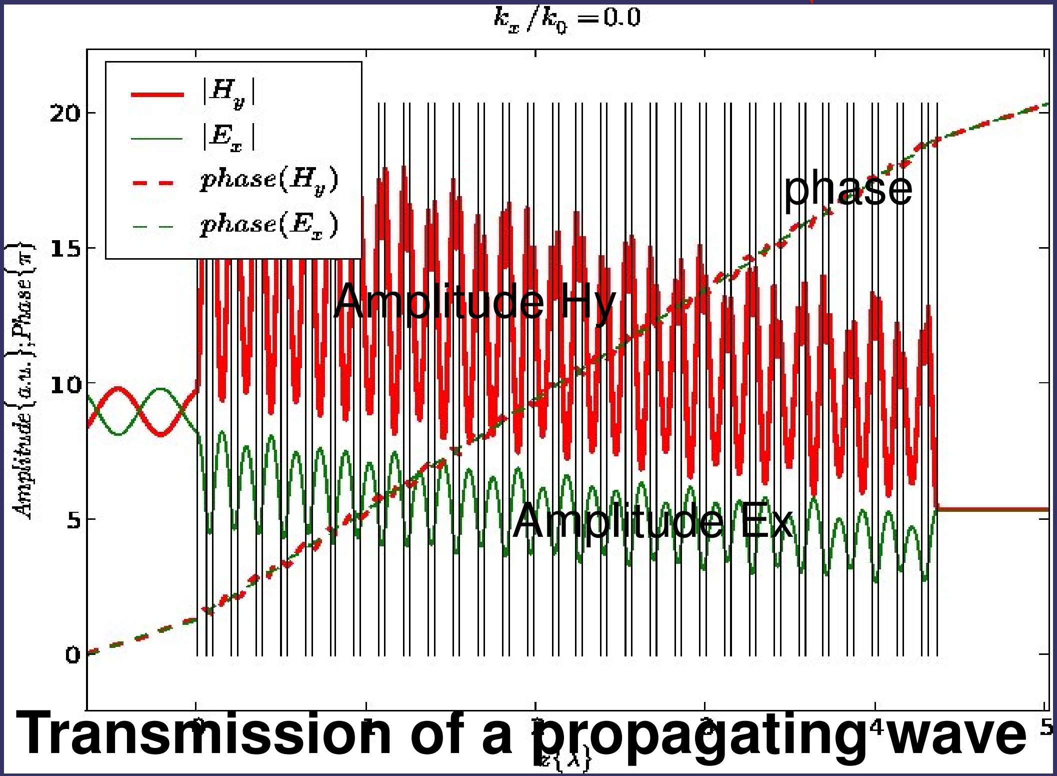

Transmission of a propagating wave

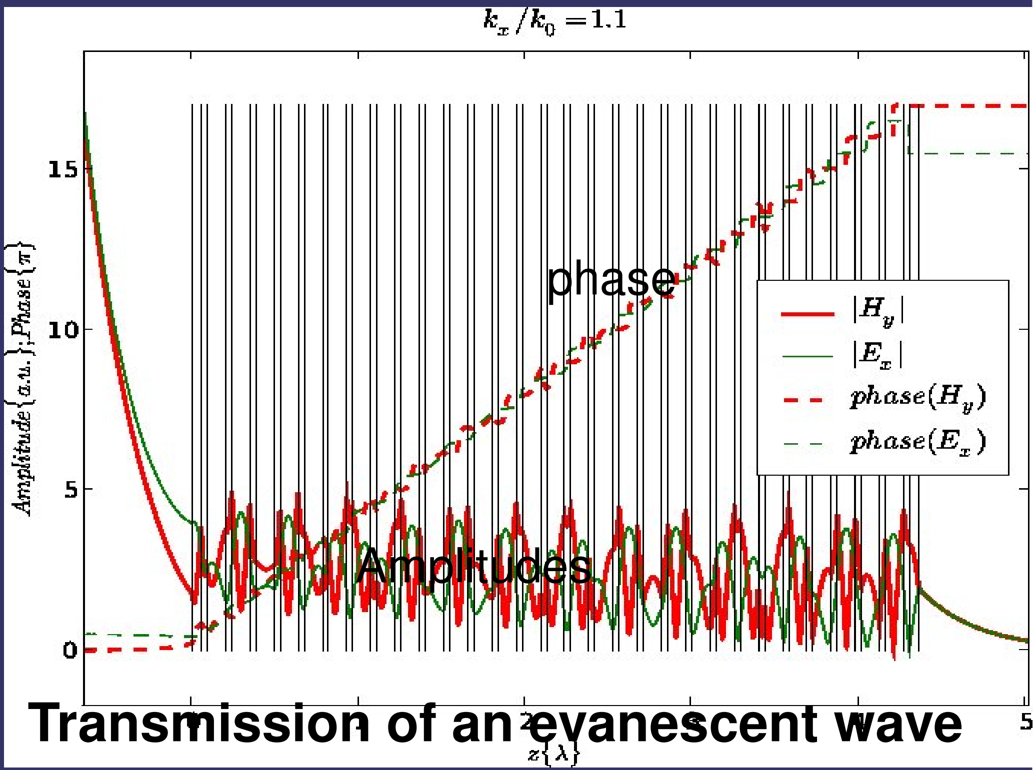

Transmission of an evanescent wave

TMM – 2D transmission (stationary state)

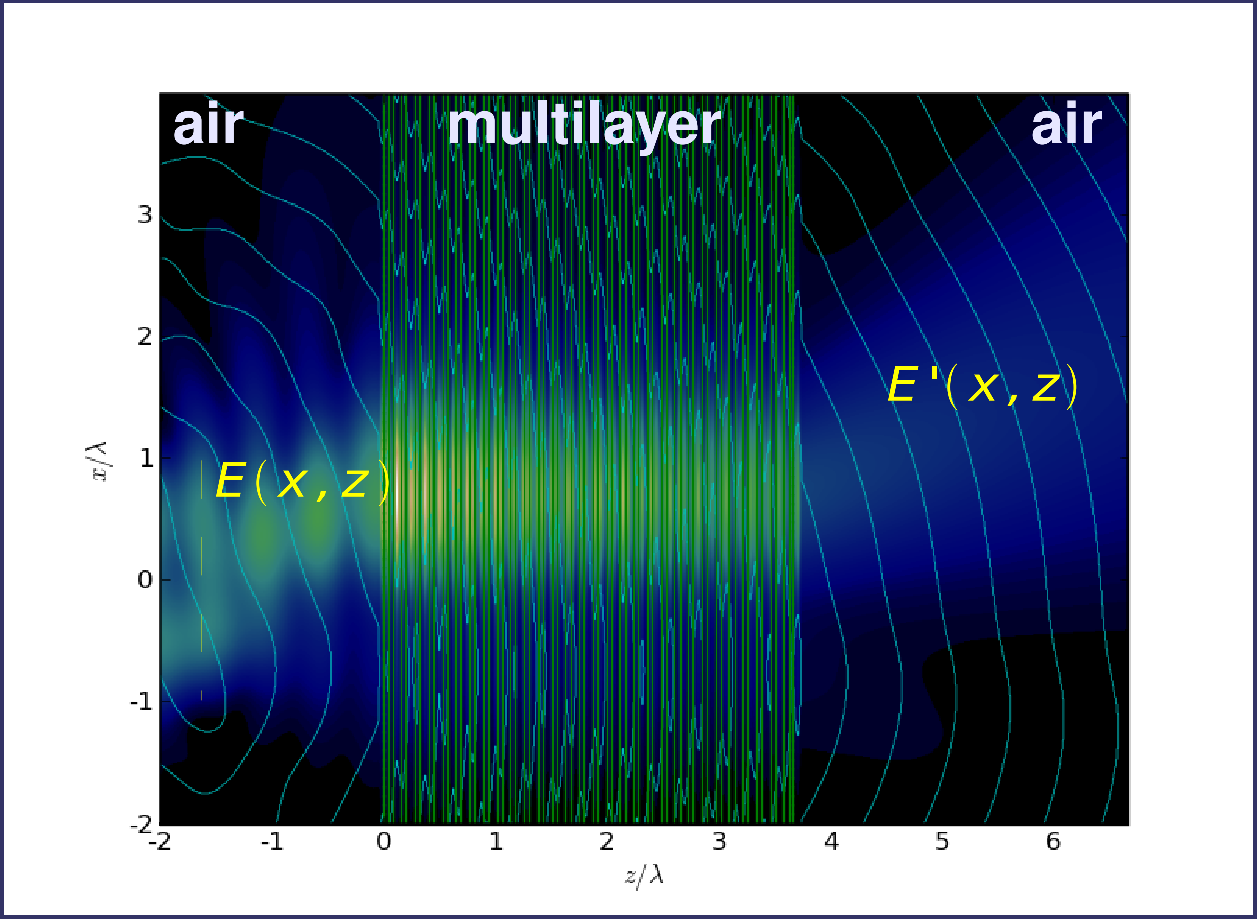

- Decomposition of the source into plane waves + TMM + reconstruction

$$E(x,z)=\int \hat{E}(k_x)\exp(ixk_x+iz\sqrt{k_0^2n^2-k_x^2})dx$$

TMM

$$E'(x,z)=\int \hat{E}'(k_x)\exp(ixk_x+iz\sqrt{k_0^2n^2-k_x^2})dx$$

- Orders of magnitude faster than FDTD

TMM – time domain simulation

Dispersive reshapement of a 1D pulse at a RHM/LHM boundary

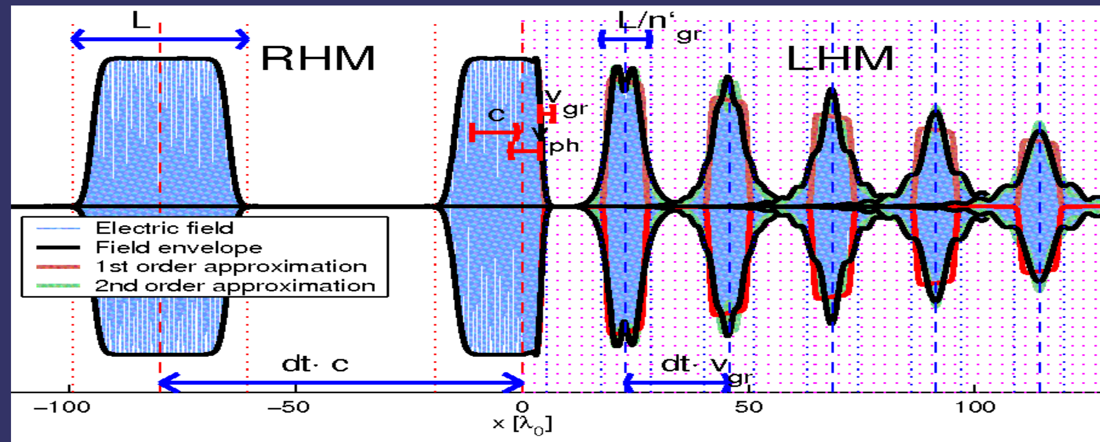

Dispersive reshapement of a 2D wavefront at a RHM/LHM boundary

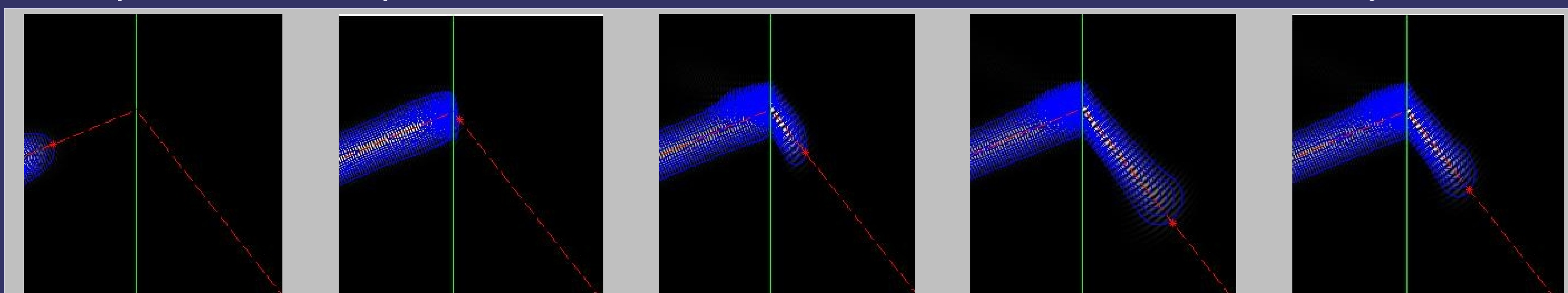

- **Decomposition of the source into plane waves + TMM + reconstruction**

$$E(x,z,t)=\Re\int\int \hat{E}(k_x,\omega)\exp(ixk_x+iz\sqrt{k_0^2n^2-k_x^2}-i\omega t)\,dx\,d\omega$$

TMM

$$E'(x,z,t)=\Re\int\int \hat{E}'(k_x,\omega)\exp(ixk_x+iz\sqrt{k_0^2n^2-k_x^2}-i\omega t)\,dx\,d\omega$$

- **Still a lot faster than FDTD**

TMM – calculation of the Modulation Transfer Function and Point Spread Function

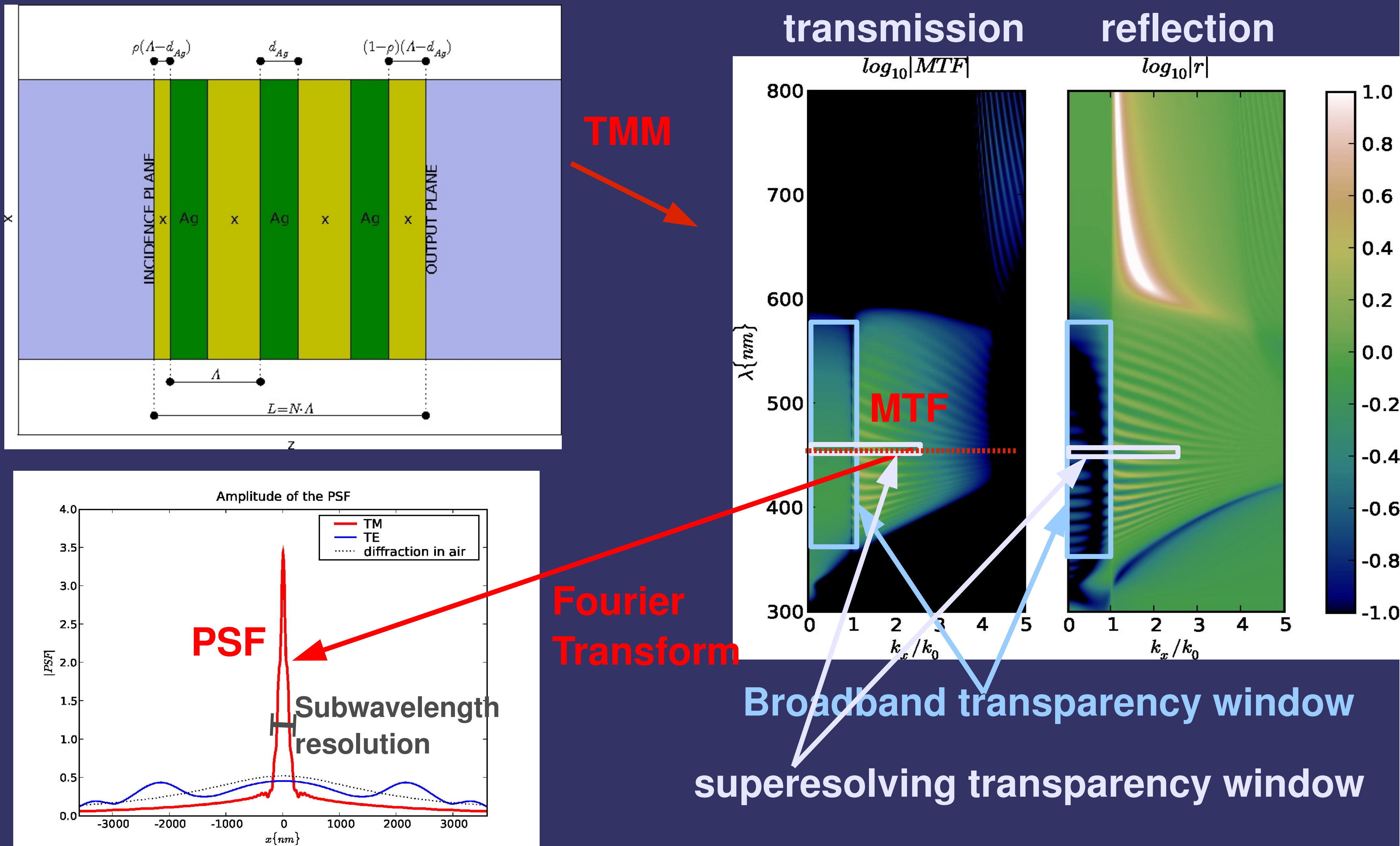

Full 3D imaging couple TE/TM spatial harmonics

Vectorial treatment:

$$E'(x,y)=H(x,y)*E(x,y)$$

vector matrix vector

$$\mathbf{H}_\sigma(\rho,\phi)=\mathbf{H}_m(\rho)\begin{bmatrix}1 & 0\\ 0 & 1\end{bmatrix}-\mathbf{H}_\delta(\rho)\begin{bmatrix}0 & \exp(2i\phi)\\ \exp(-2i\phi) & 0\end{bmatrix}$$

Fourier-Bessel Transform of $(\hat{H}_{TM}+\hat{H}_{TE})/2$

2nd order Hankel Transform of $(\hat{H}_{TM}-\hat{H}_{TE})/2$

Example: polarisation coupling in 2D for a circularly polarised point signal (imaging through 5 Ag-air 80nm layers)

Unchanged polarisation Orthogonal polarisation

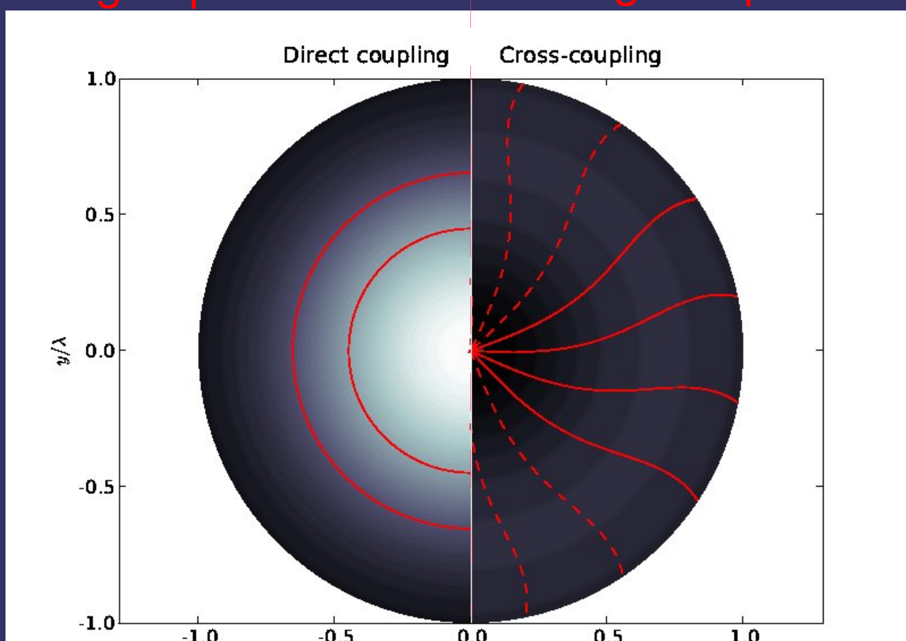

PSF Intensity + phase isolines (every pi/4)

Spatial representation

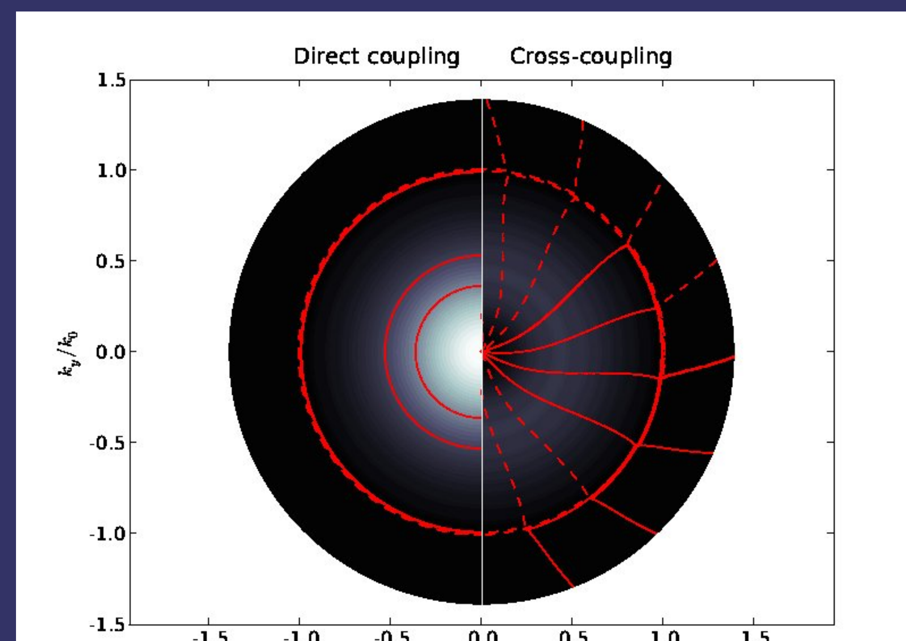

MTF Intensity + phase isolines (every pi/4)

Spatial frequency representation

1. Subwavelength imaging (superresolution)

Silver superlens

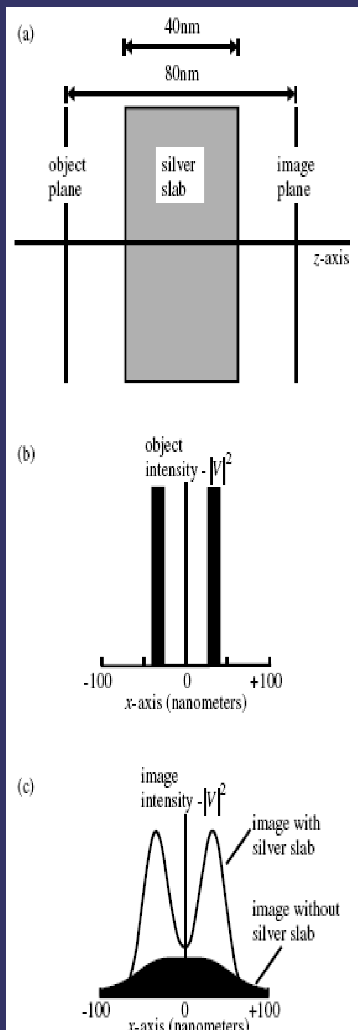

J.B. Pendry, Phys. Rev. Lett. 85, 3966, *Negative refraction makes a perfect lens* (2000)

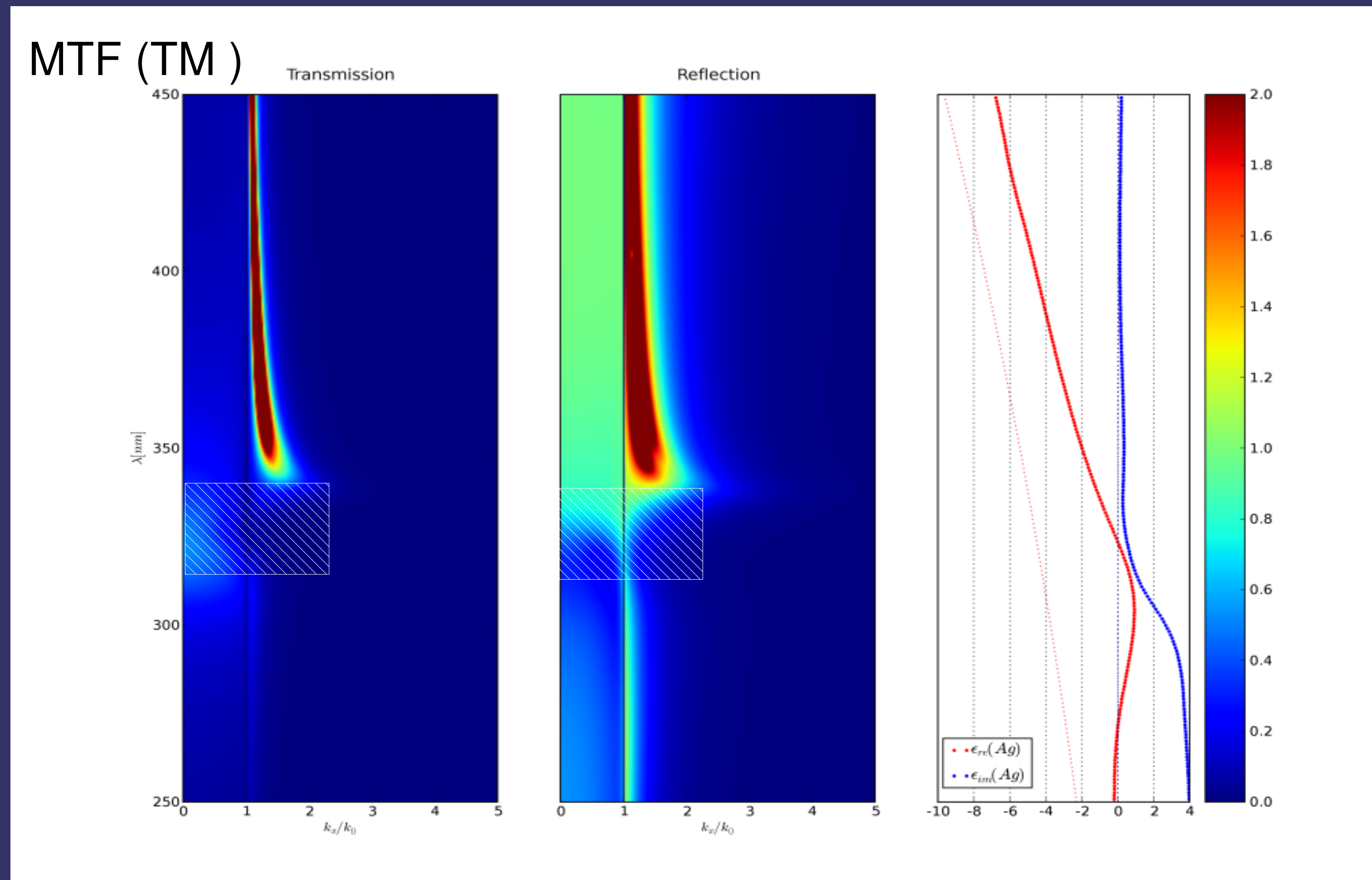

- Operation near the cut-off
- Evanescent wave enhancement with SPP
- Effective permittivity (EMT): $\overline{\epsilon_{\parallel}^{EMT}} = 0 \, , \overline{\epsilon_{\perp}^{EMT}} = \infty$

Point Spread Function of the silver superlens

$$H(x) = \frac{1}{2\pi} \int \hat{H}_{TM}(k_x) \exp(i k_x x) dk_x$$

Problems due to singularities of the MTF

$$PV \int \frac{1}{|k_x| - k_s} \exp(i k_x x) dk_x \longrightarrow \propto -\sin(k_s |x|)$$

MTF PSF

Dependence of the PSF

- on losses
- on slab thickness

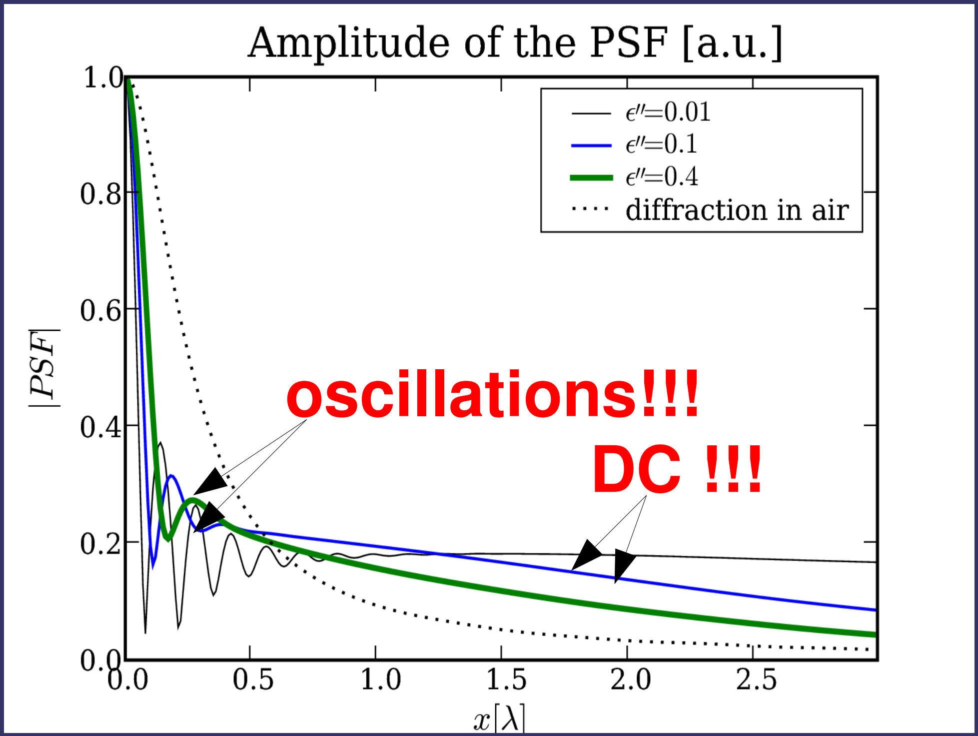

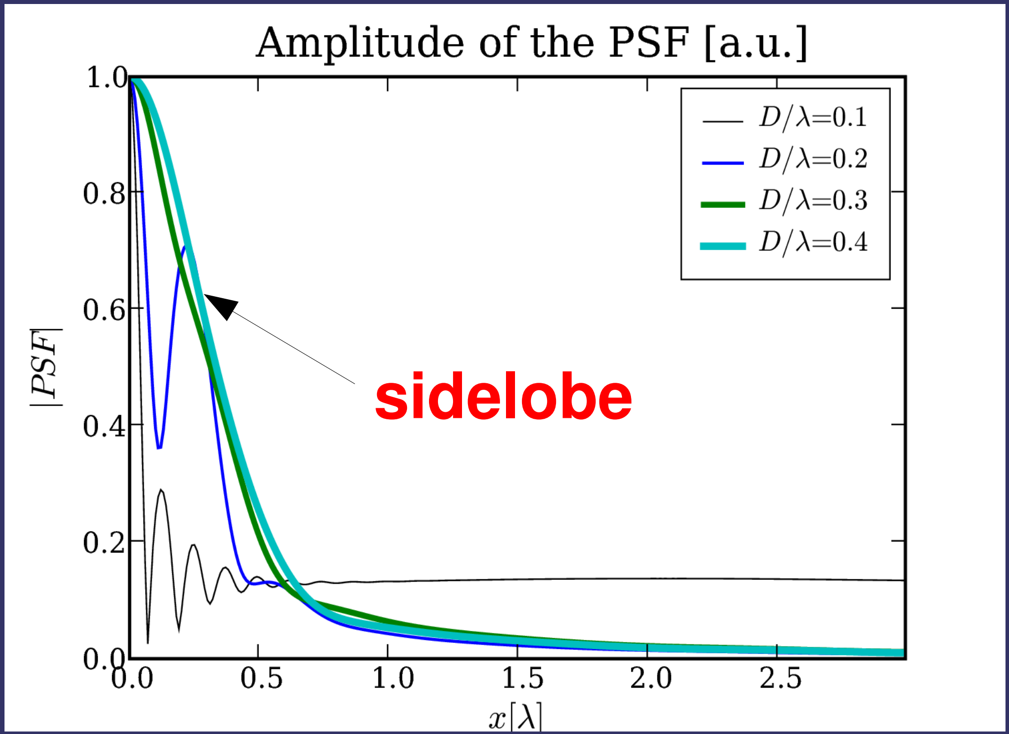

1. Subwavelength imaging (superresolution)

Resonant tunnelling

M. Scalora et al. "Negative refraction and sub-wavelength focusing in the visible range using transparent metallo-dielectric stacks" Opt Expr., **15**, 508, 2007.

M. Scalora et al. "Transparent metallo-dielectric one dimensional photonic band gap structures" Appl. Phys., **83**, 2377, 1998.

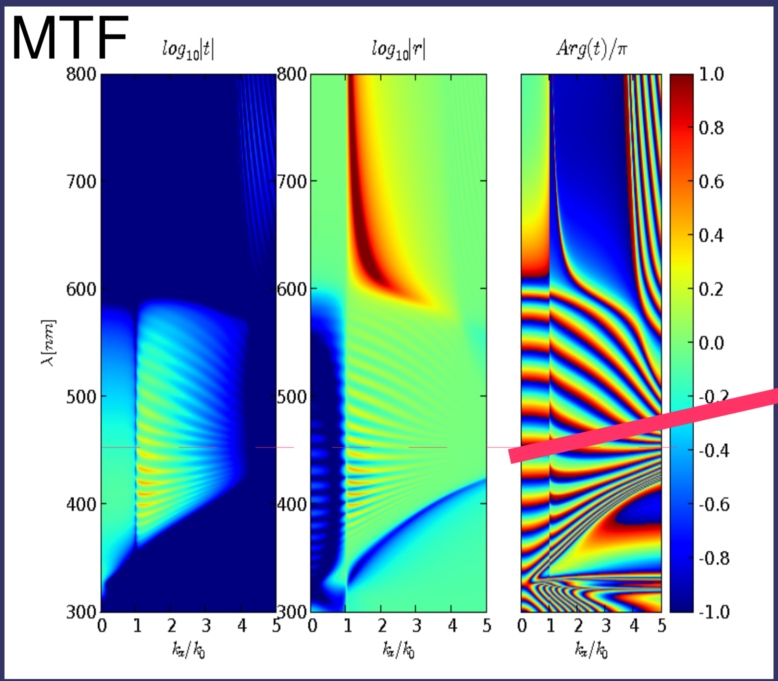

Transparency range

٣٧٠nm – 560nm

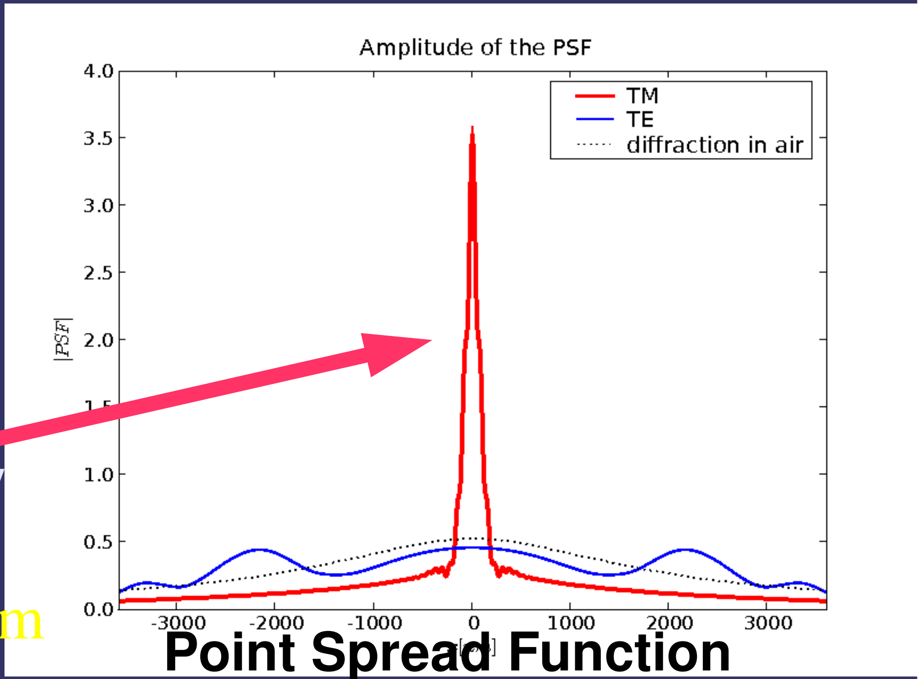

L=1650nm $\epsilon_1=\epsilon_{Ag}, \epsilon_2=8, N=30, d_1=20\text{nm}, d_2=35\text{nm}$

Resonant tunnelling

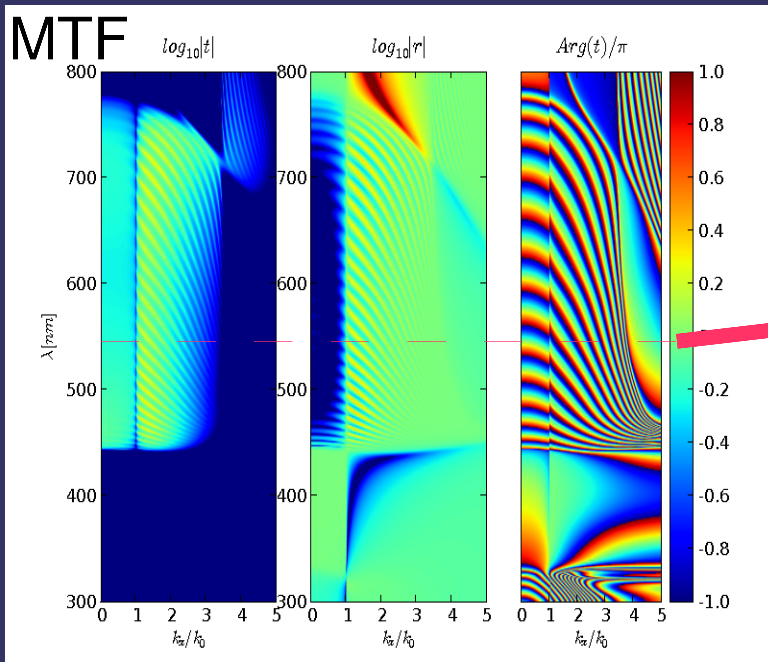

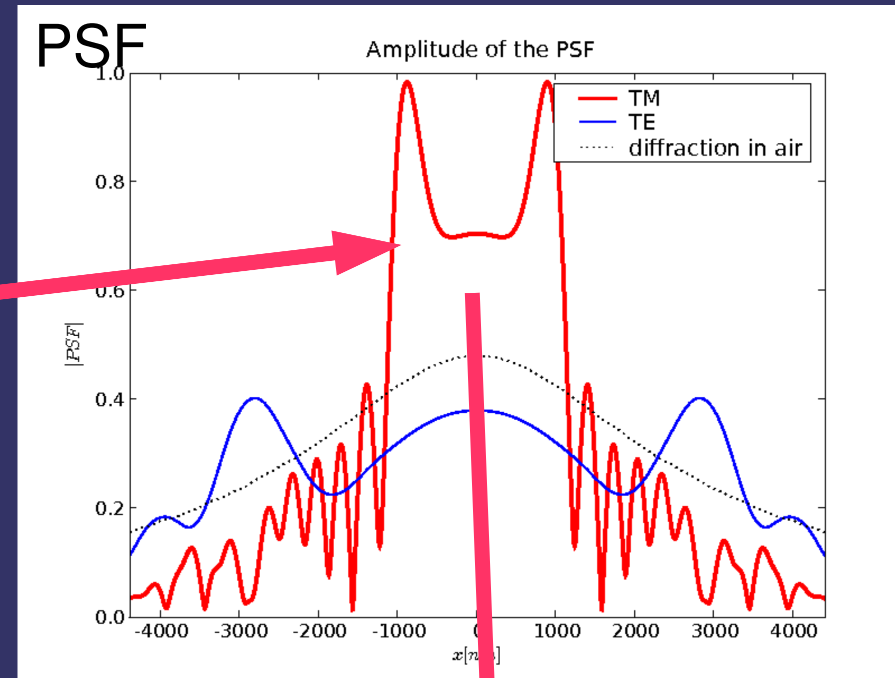

L=2400nm $\epsilon_1=\epsilon_{Ag}, \epsilon_2=8, N=30, d_1=20\text{nm}, d_2=60\text{nm}$

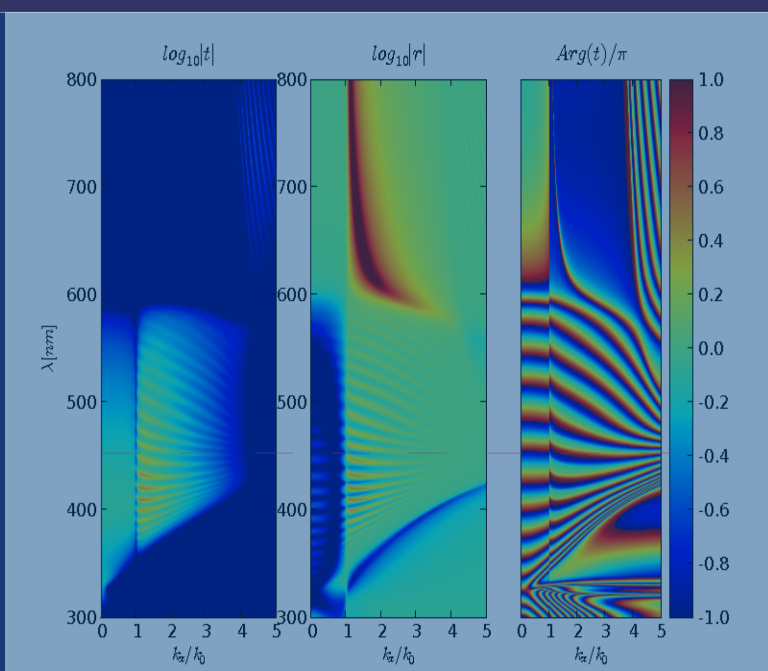

L=1650nm $\epsilon_1=\epsilon_{Ag}, \epsilon_2=8, N=30, d_1=20\text{nm}, d_2=35\text{nm}$

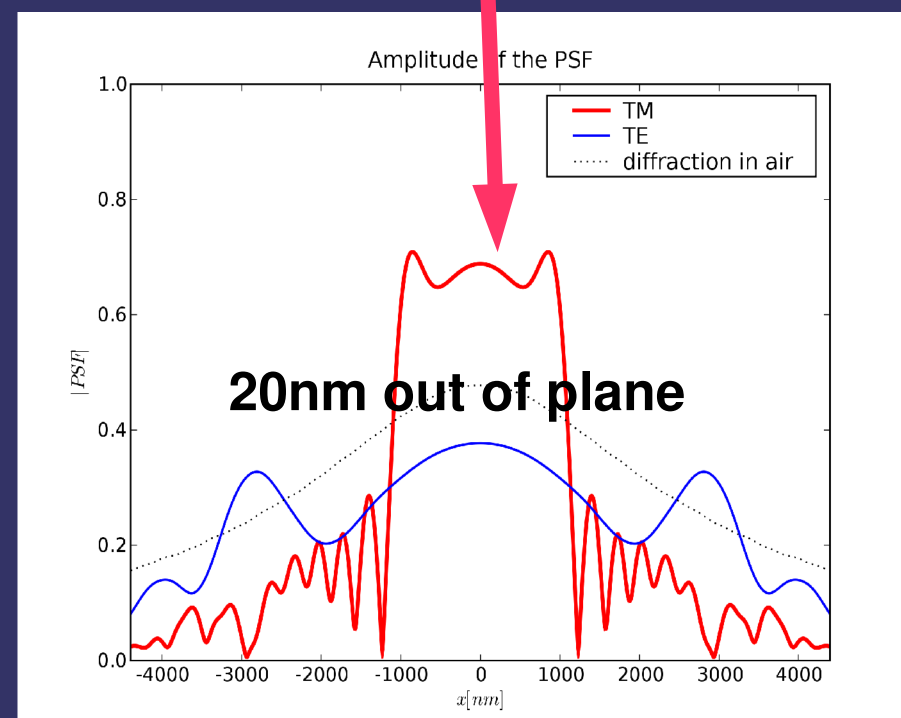

1. Subwavelength imaging (superresolution)

Canalization

P. Belov, Y. Hao, Phys Rev. 73, 113110 (2006)

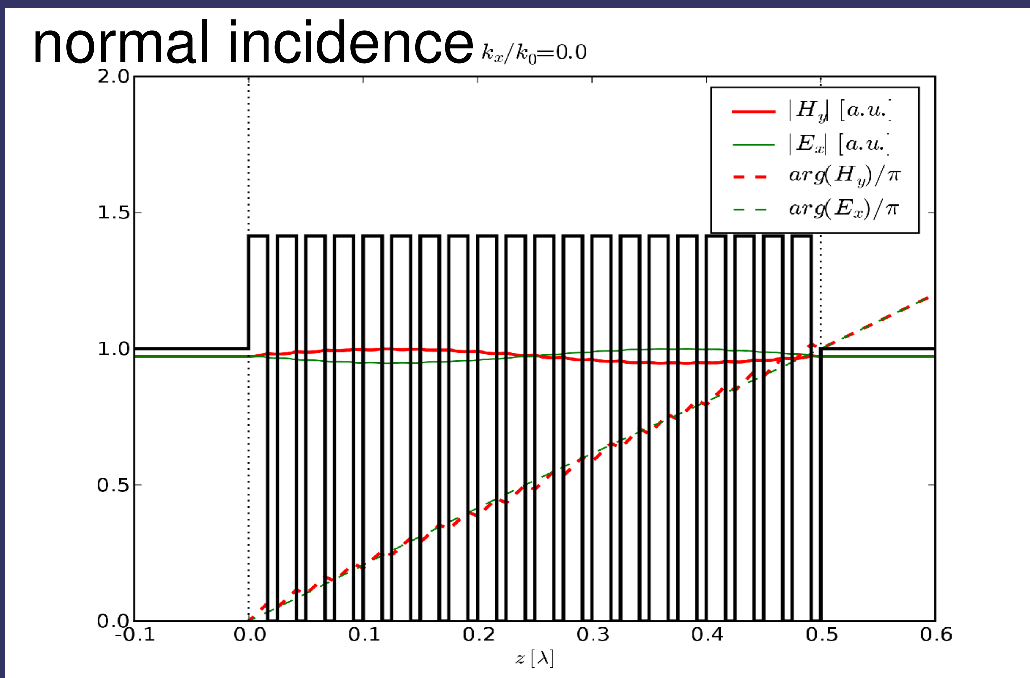

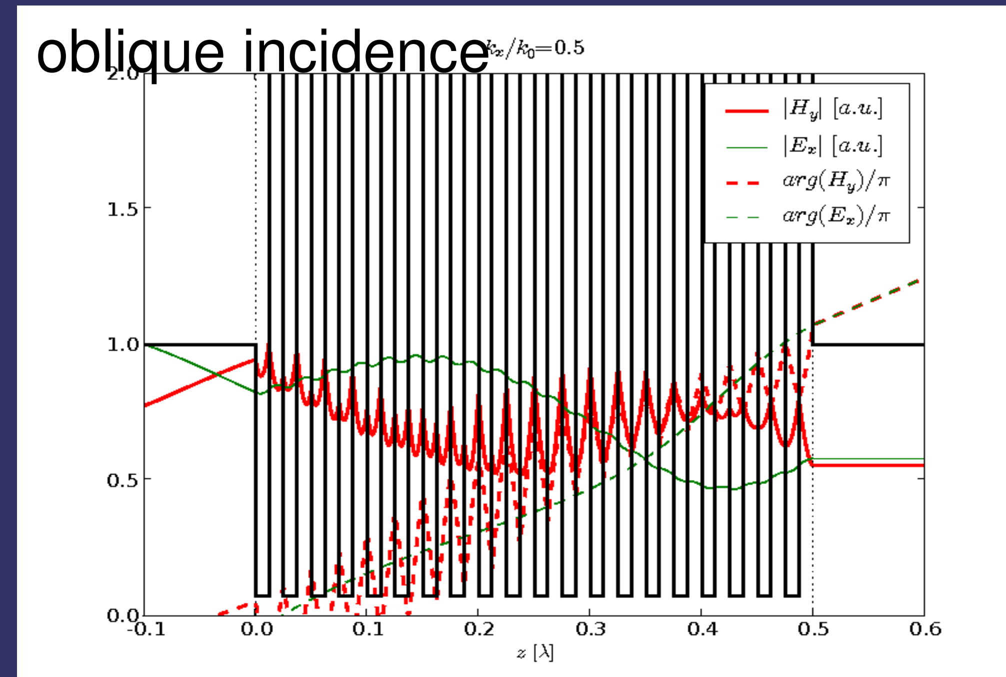

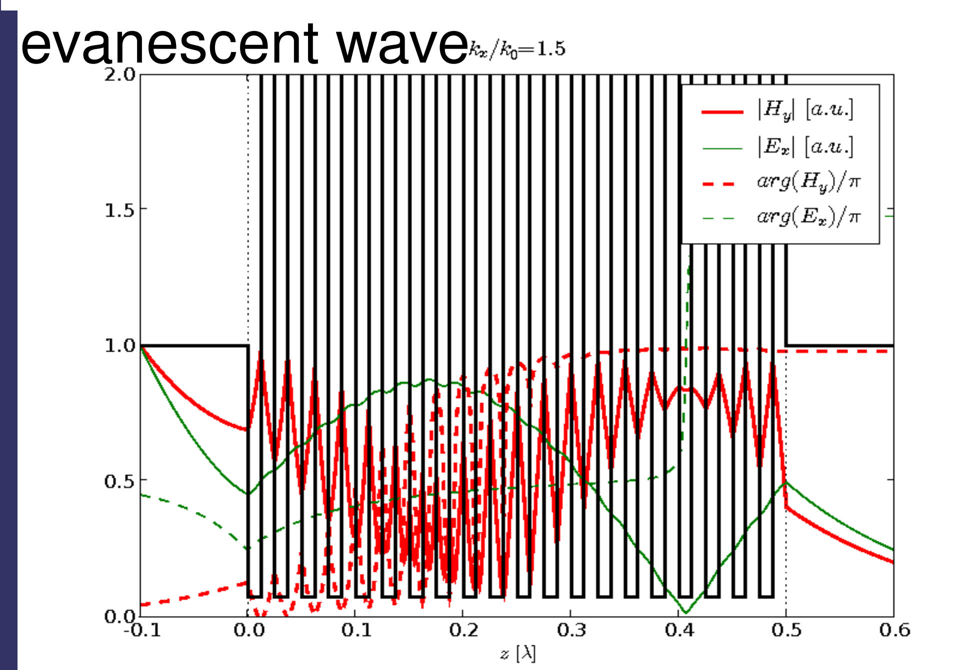

The same FP resonant condition for any angle of incidence and for a range of evanescent waves!

$$L/\lambda = m/2$$

Regime (EMT): $\overline{\epsilon_{\parallel}^{EMT}} = 1, \overline{\epsilon_{\perp}^{EMT}} = \infty$

Canalization regime – lossless case

Idealised, **lossless** conditions:

$$\overline{\epsilon_{\parallel}^{EMT}}=1,\ \overline{\epsilon_{\perp}^{EMT}}=\infty,\ L/\lambda=m/2$$

Modulation Transfer Function

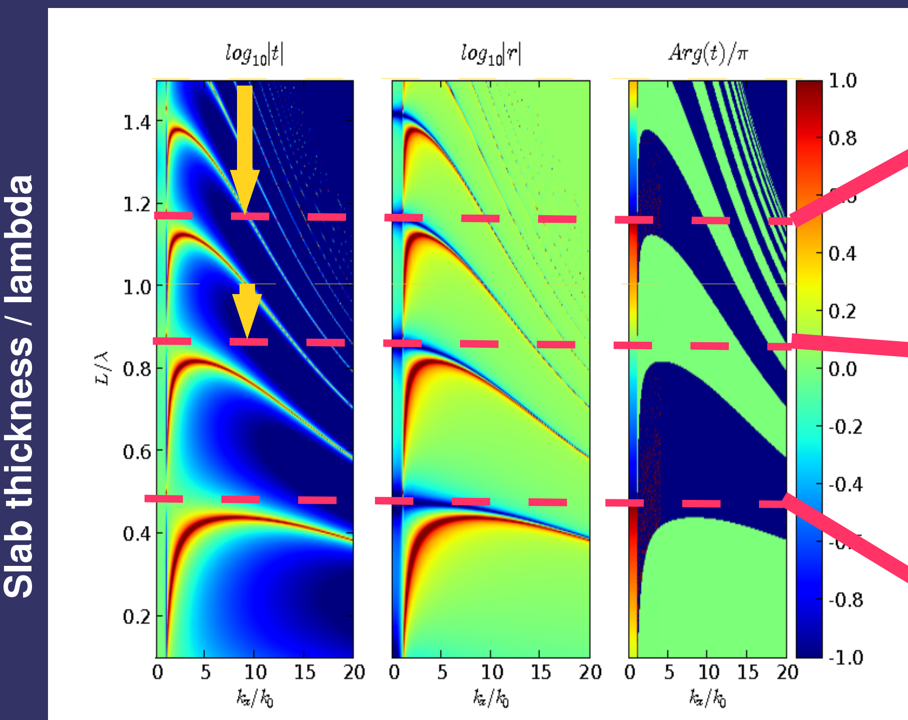

$\epsilon_{Ag}=-14.68, \epsilon_x=15.68, N=20$

Point Spread Functions

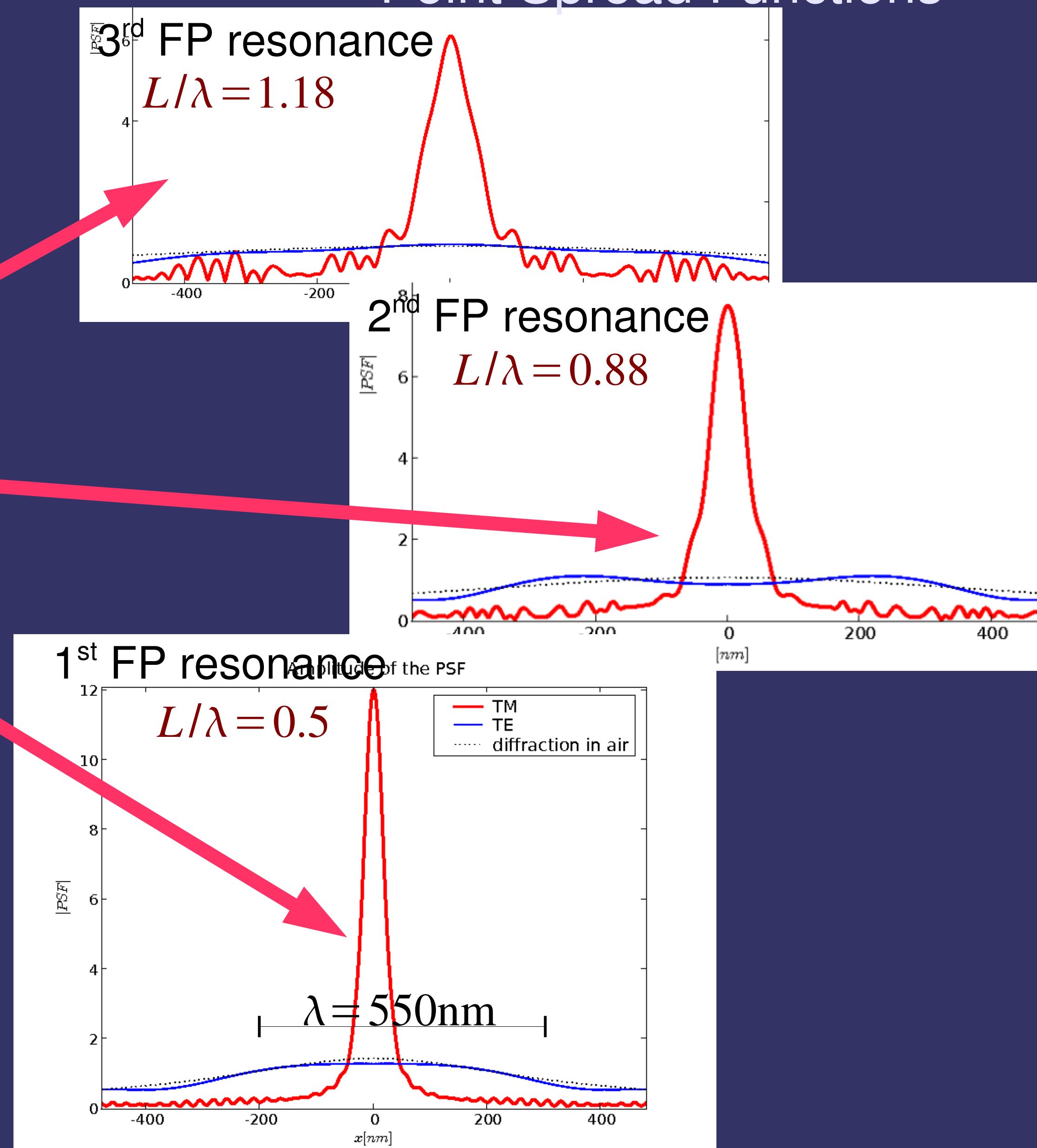

Canalization regime - with losses

$\epsilon_{Ag} = -14.68$

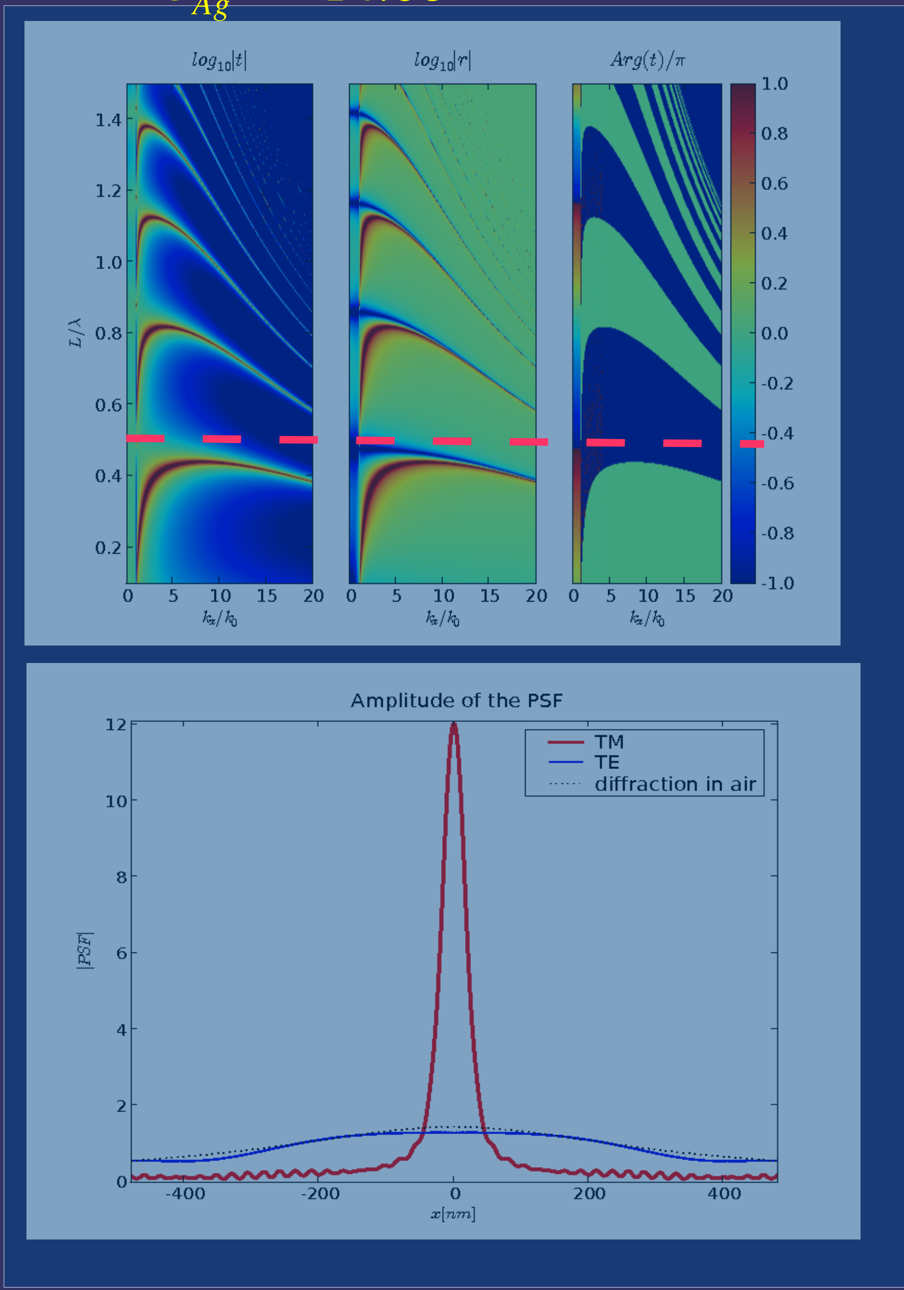

$\epsilon_{Ag} = -14.68 + 0.65i$

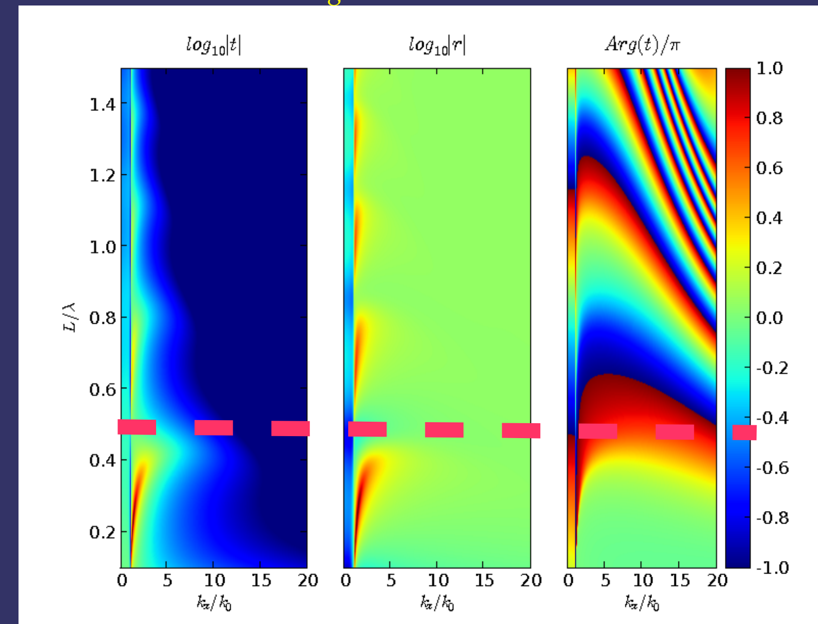

1st FP resonance

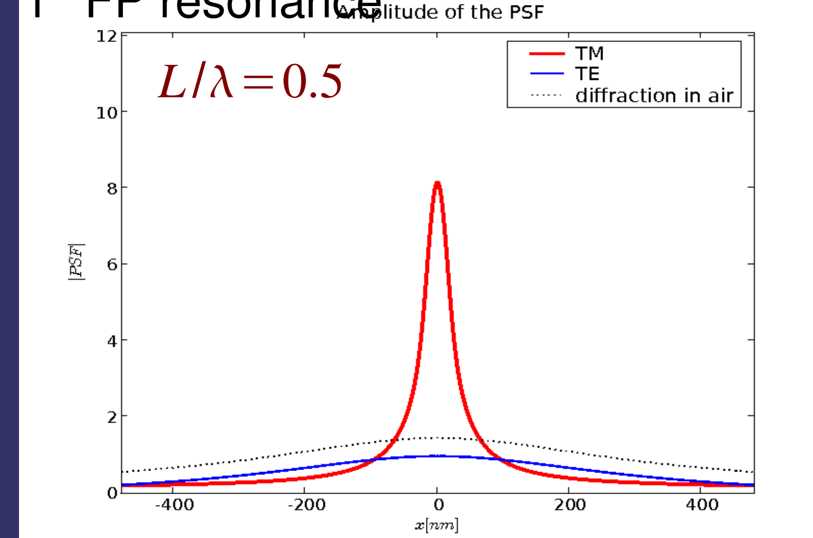

2. Laplace filtering

- 1D Laplace filter

$$H(x) = 2\delta(x) - \delta(x-\epsilon) + \delta(x+\epsilon)$$

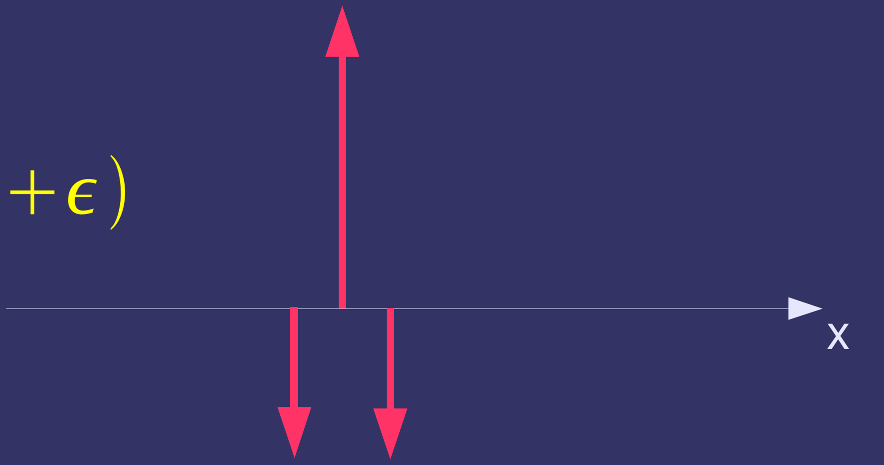

- 2D discrete Laplace filter:

$$H_{ij} = \begin{bmatrix} 0 & -1 & 0 \\ -1 & 4 & -1 \\ 0 & -1 & 0 \end{bmatrix}$$

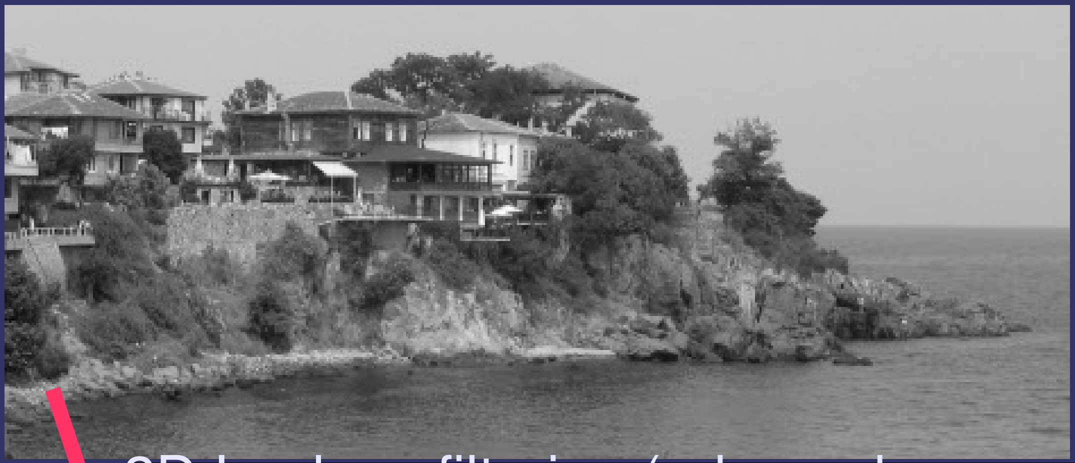

2D Laplace filtering (edge enhancement)

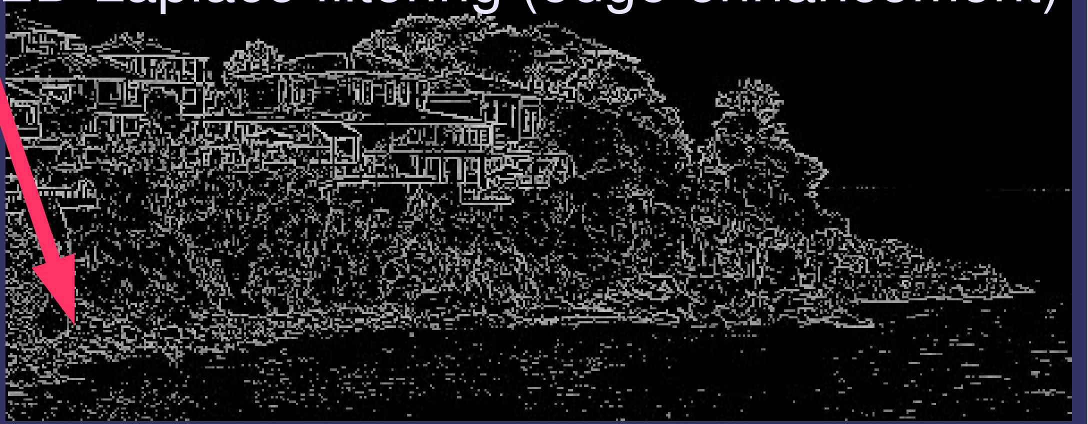

Optimization of the multilayer with respect to the MTF

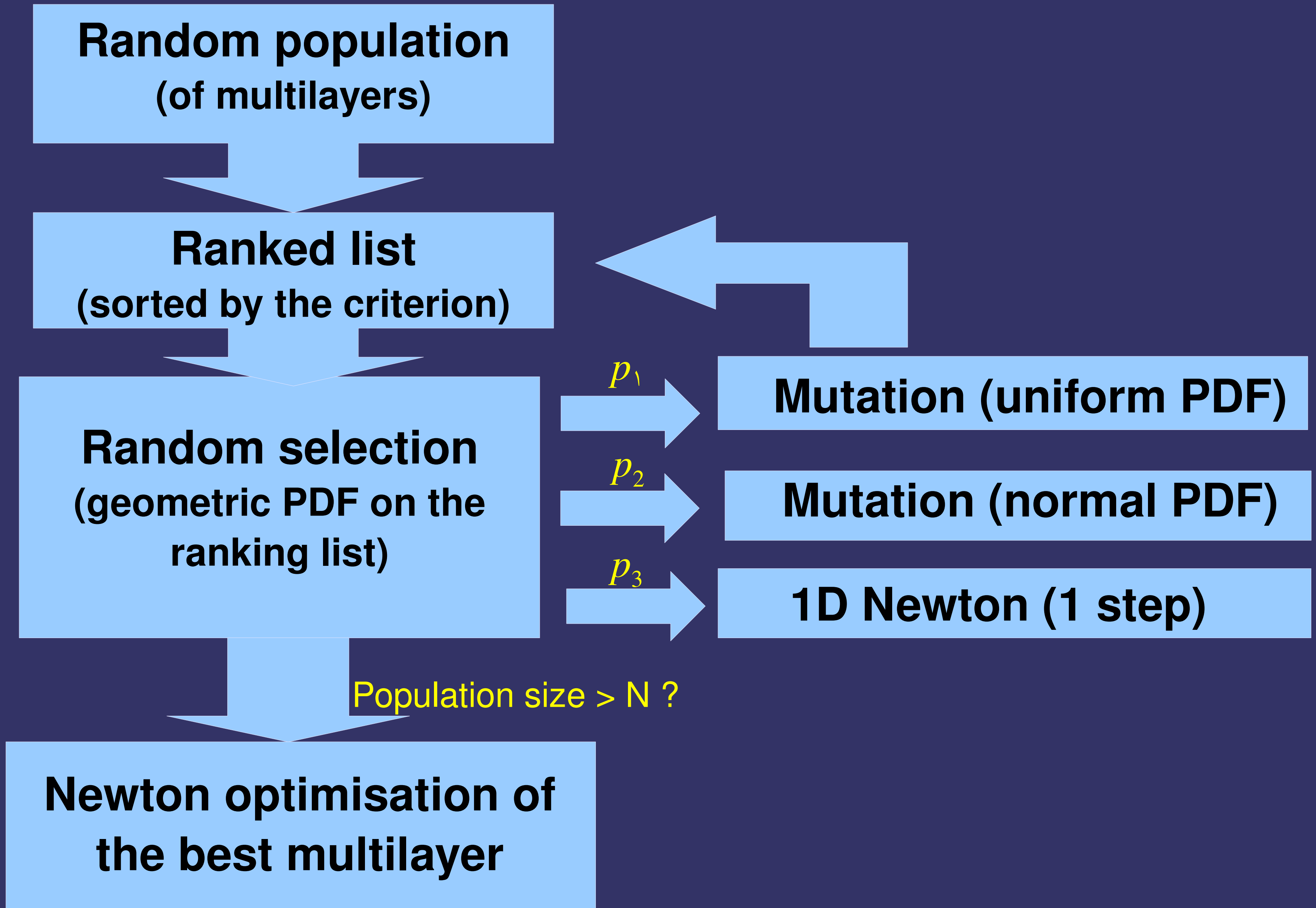

Optimization of the multilayer for Laplace filtering

Optimised structure

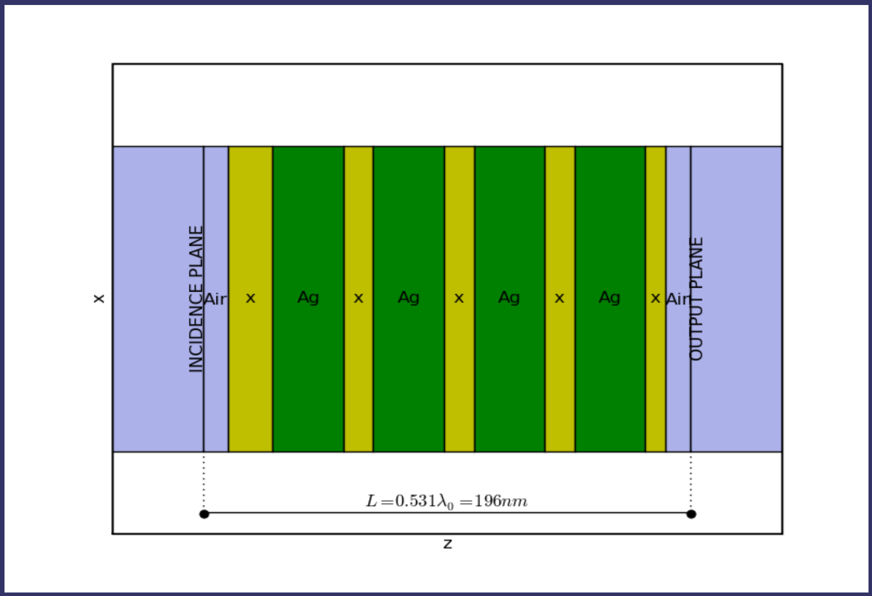

Formulation of the criterion:

Desired MTF: $\hat{H}(k_x) = (1-\cos(\eta_s k_x))\cdot e^{\frac{-k_x^2}{\eta_v}}$

Light efficiency: $\overline{|\hat{H}|}_{mean} \geq \eta_m$

SPP suppression: $max(|\hat{H}|) \leq \eta_{max}$

Point Spread Function

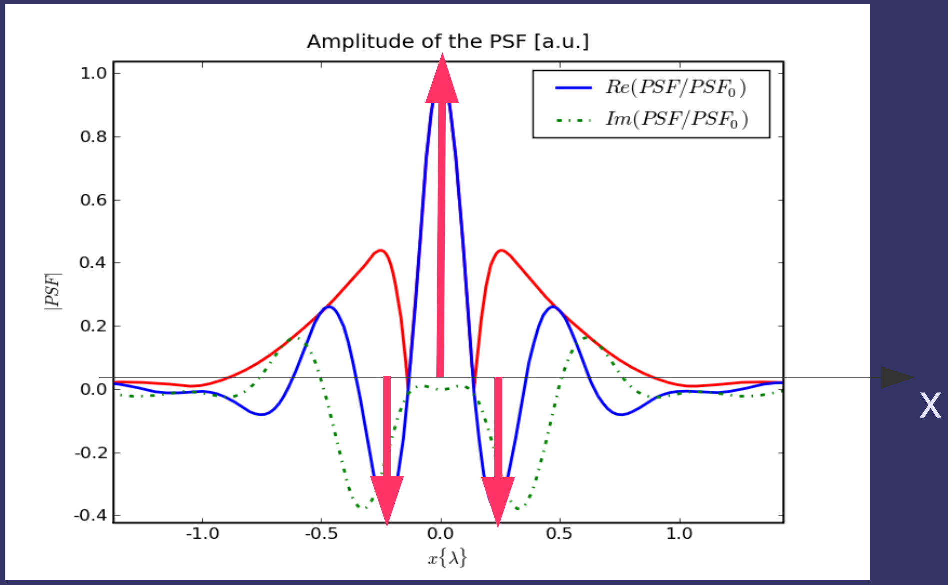

Transformation of the incident

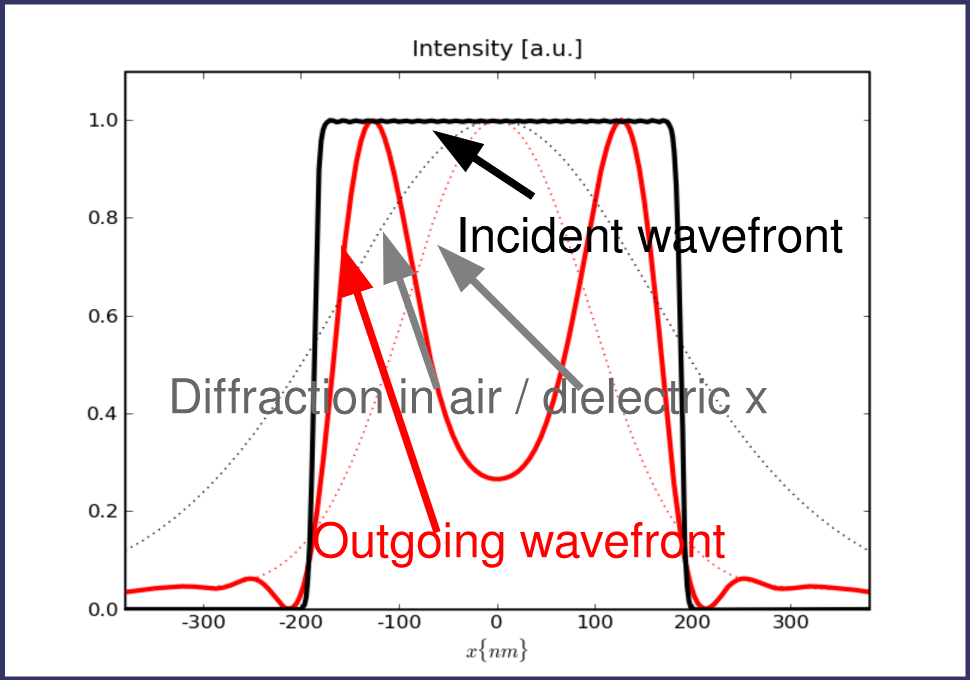

2. Laplace filtering (and subwavelength imaging)

Asymmetric flat lens

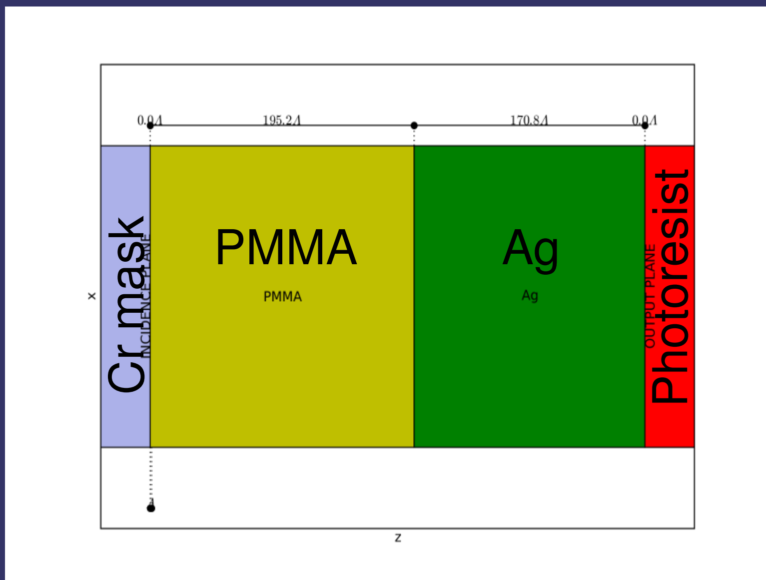

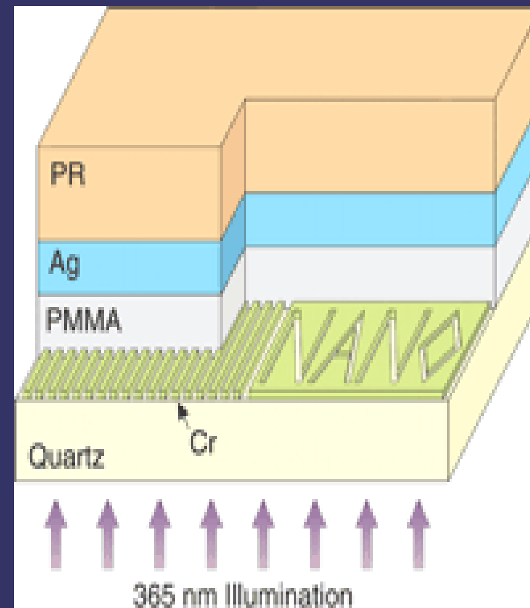

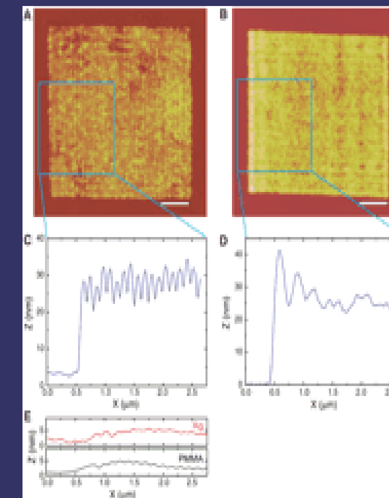

Experimental demonstration: Fang, Lee, Sun, Zhang, Science 2005, and Melville, Blaikie

Modulation Transfer Function

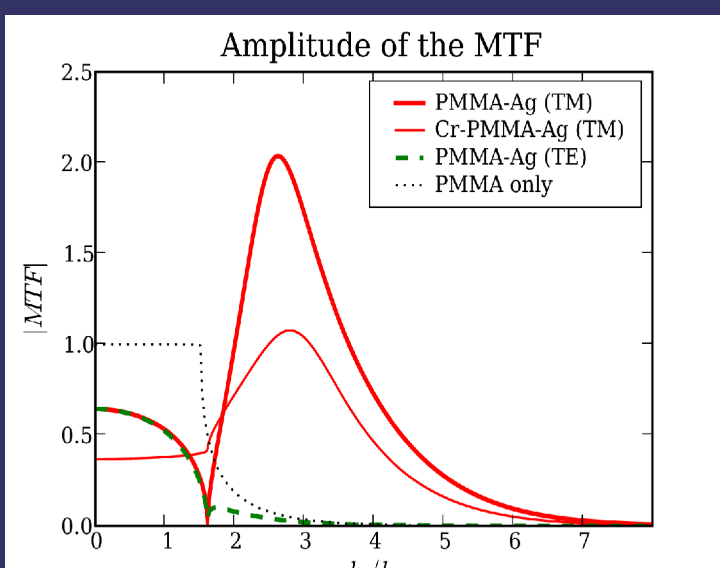

PSF (Laplace spatial filter)

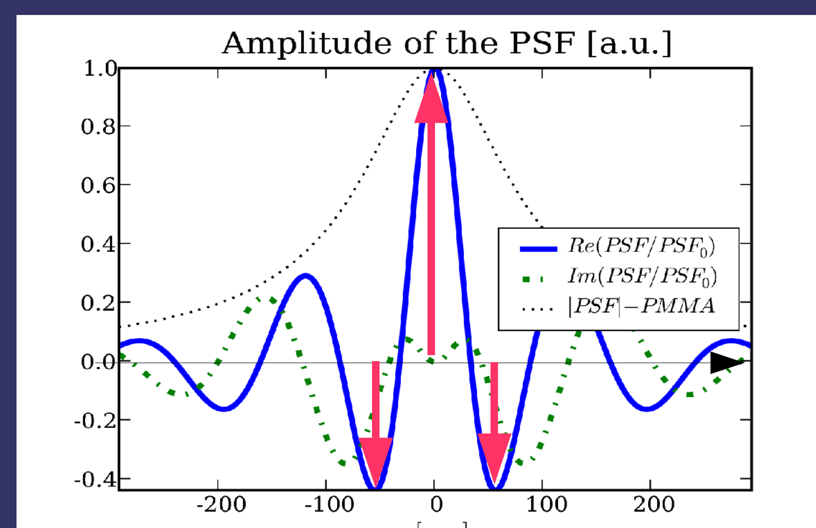

Response of the asymmetric lens to optical signals of different width

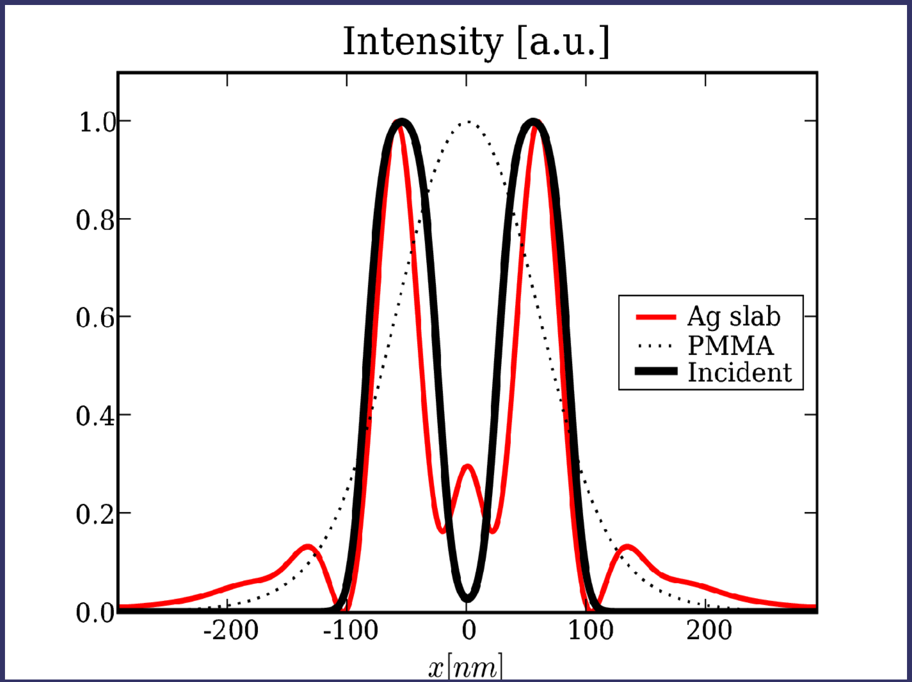

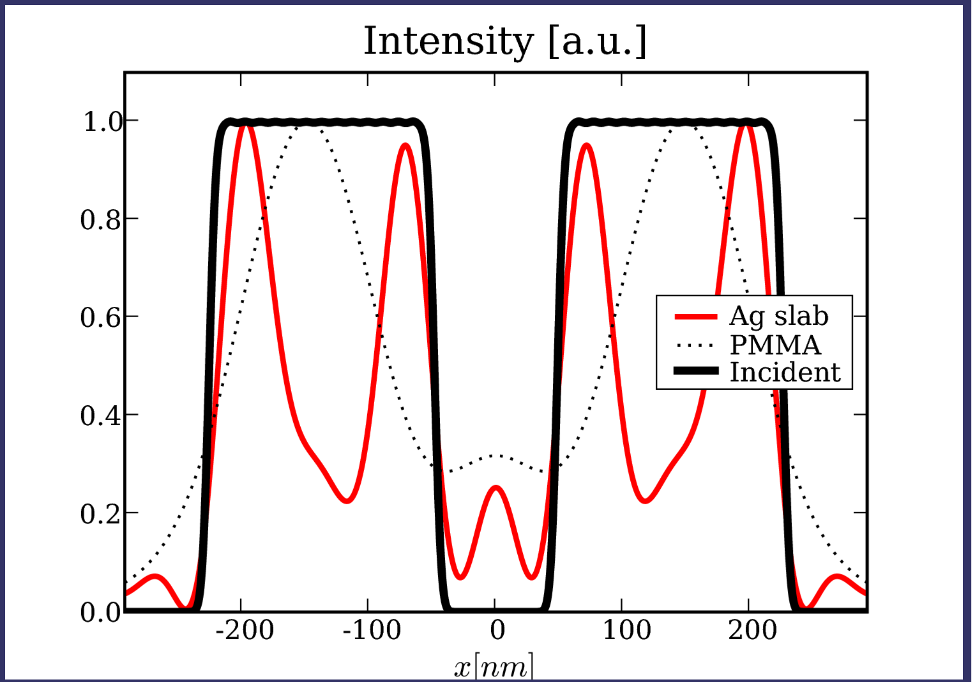

Sub-wavelength imaging

Laplace filtering

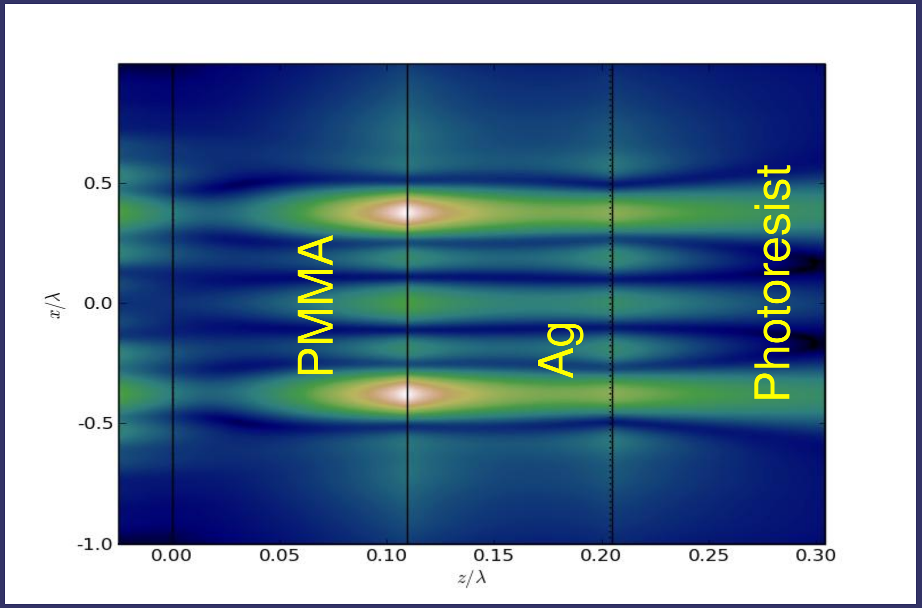

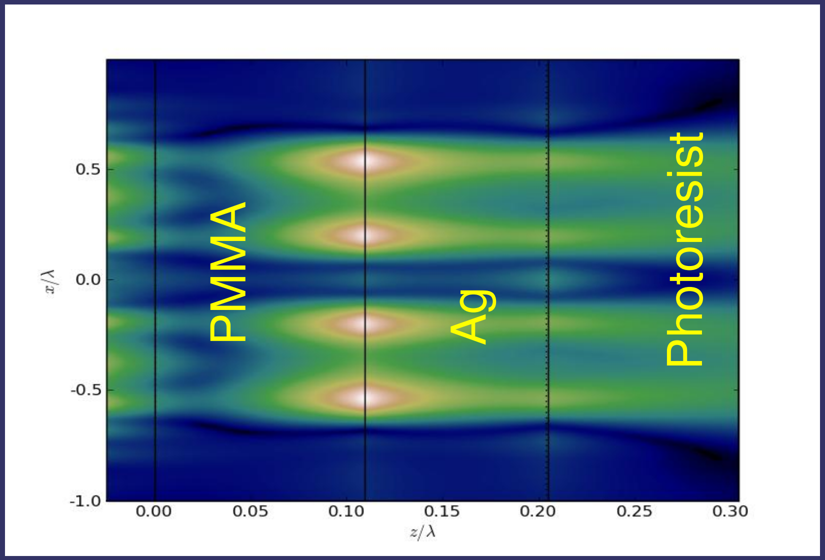

Response of the Ag-air multilayer to a rectangular incident signal

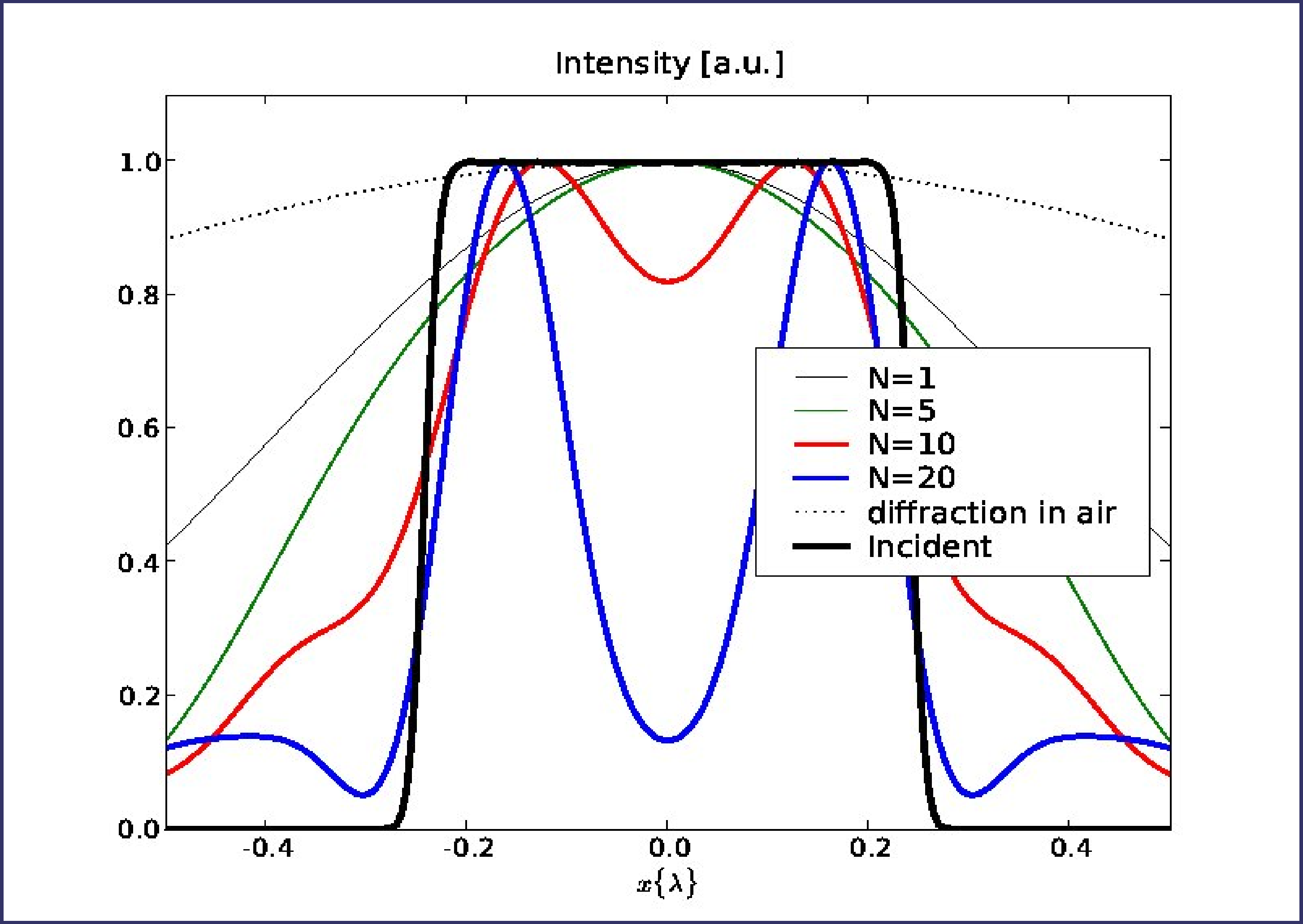

Response varies with the number of layers from imaging to Laplace filtering

Optimisation for positive and negative diffraction

MTF with a positive phase slope

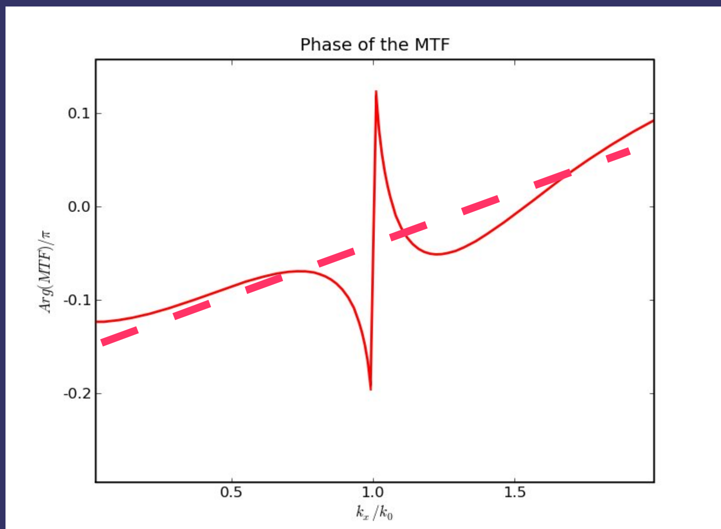

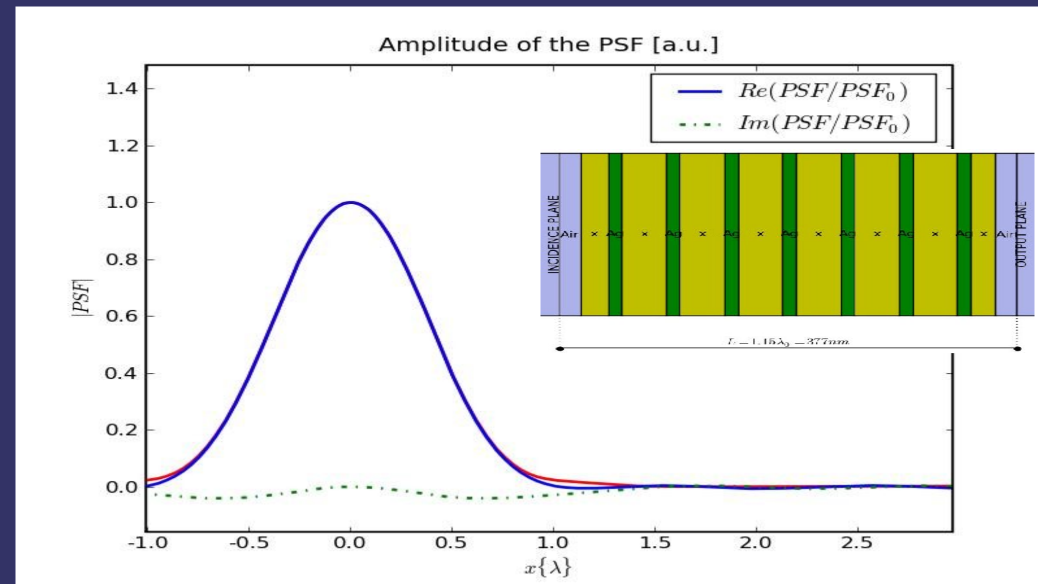

MTF with a negative phase slope

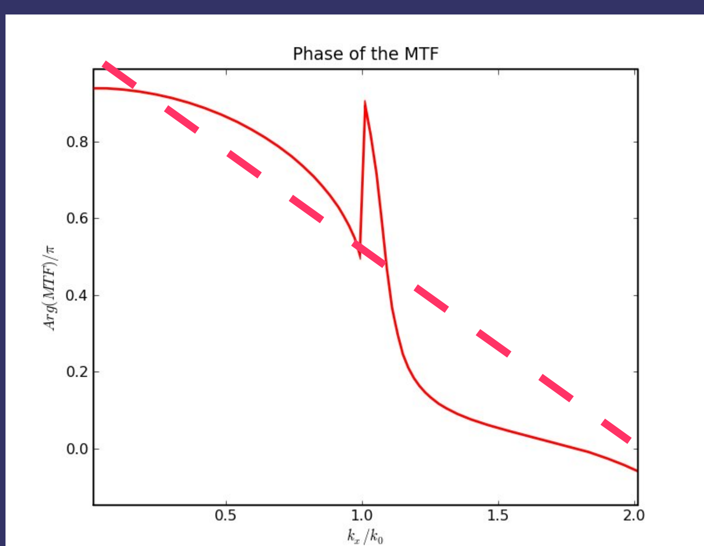

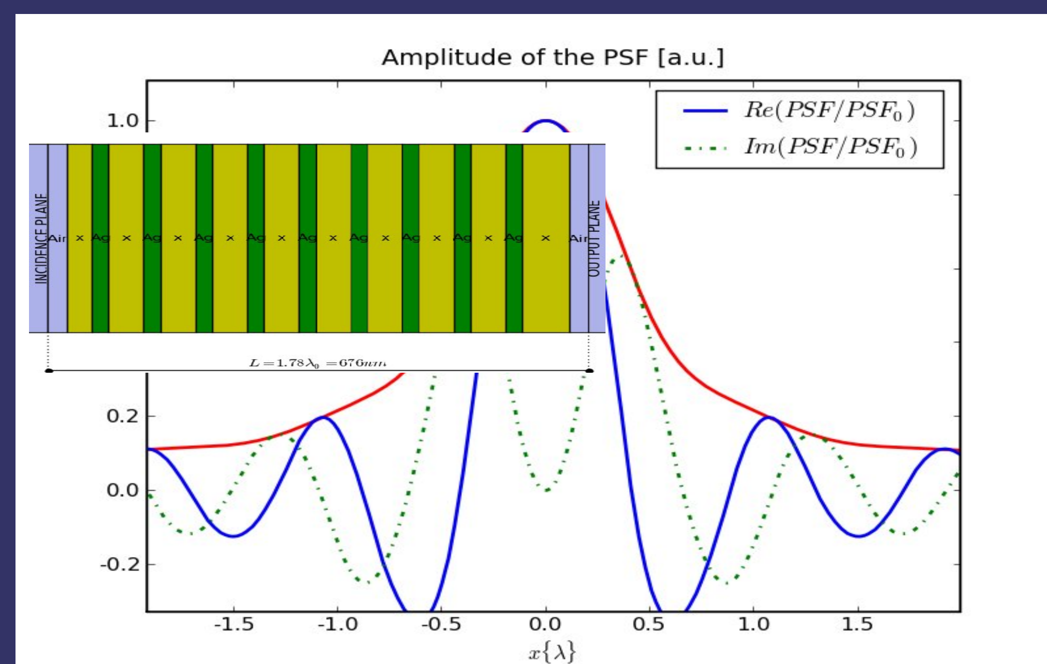

Optimisation for a phase-compensated response

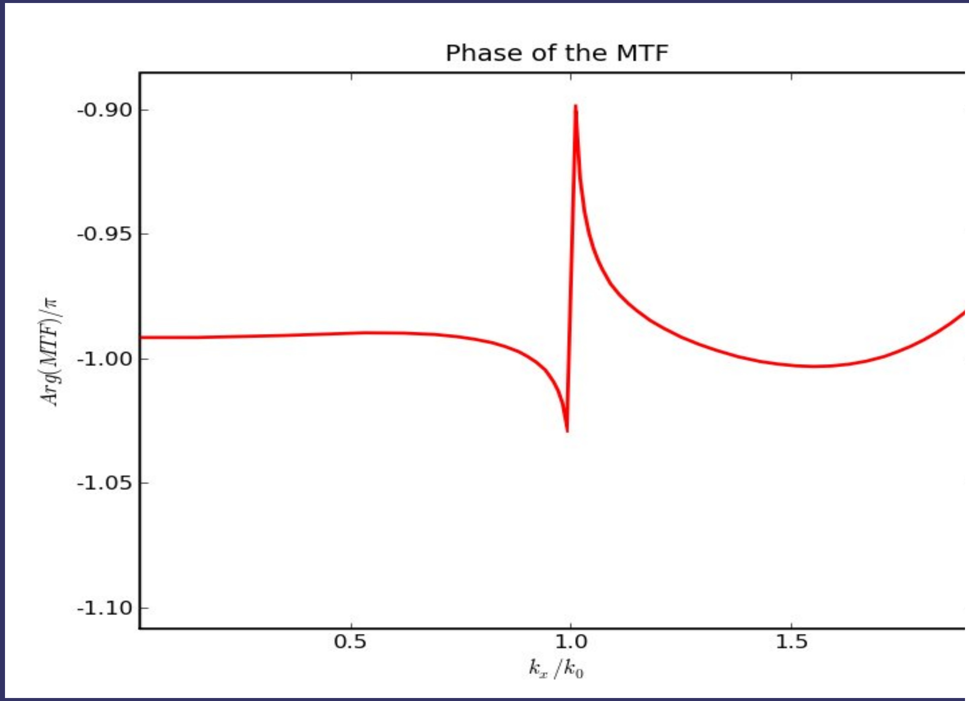

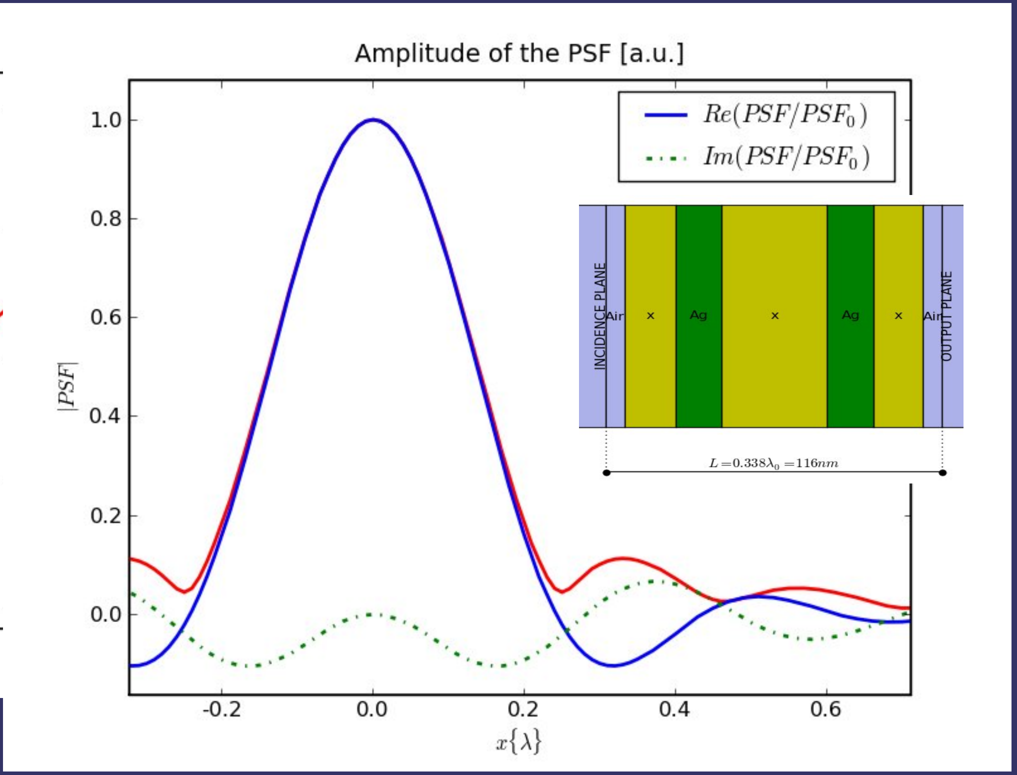

- the width of the response is sub-wavelength
- however phase of Fresnel diffraction is compensated by the multilayer

Conclusions

Summary of the numerical method:

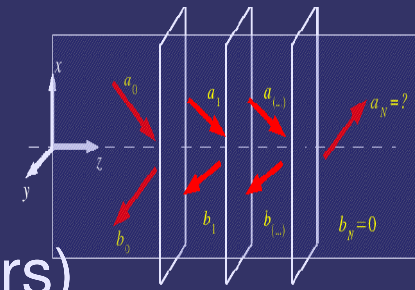

- Transfer Matrix Method → for arbitrary multi-layers
  (with lossy, dispersive, metallic, magnetic, or LHM layers)

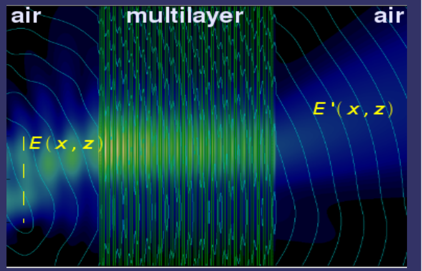

- Field decomposition / reconstruction into plane-wave representation (spatial and spectral FT; compatible with modal solvers)

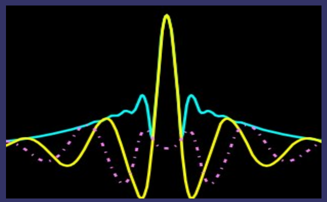

- 1D Point Spread Function computation (spatial FT of the MTF)

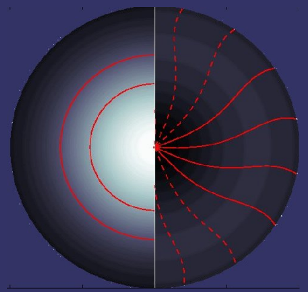

- 2D Point Spread Function computation (0^{th} and 2^{nd} order Hankel Tr.)

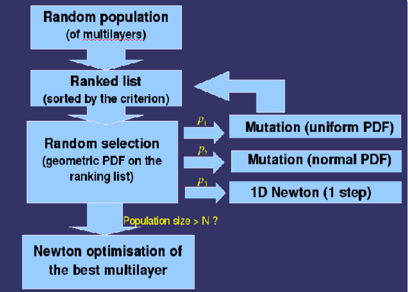

- Optimization of the multilayer with respect to the desired field transformation (Newton + random search)

Conclusions

Summary of results:

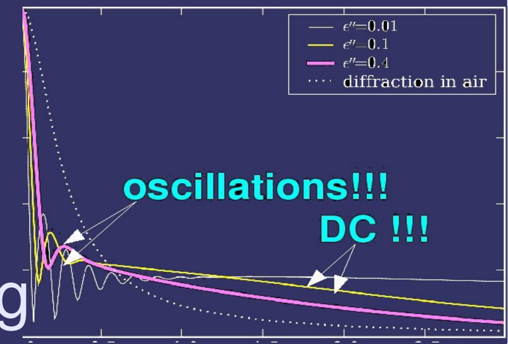

- Singularities of the MTF introduce artefacts to imaging (DC, sidelobes, differential behaviour). Losses regularise the imaging system.

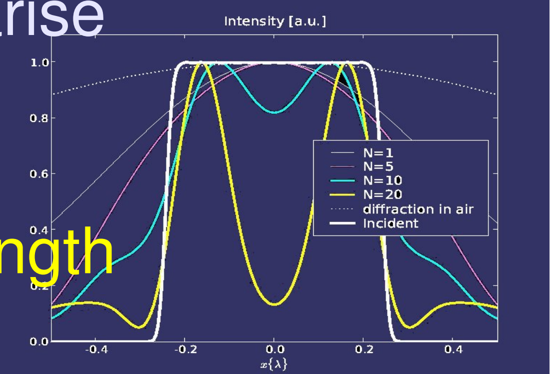

- Multilayers can be used for imaging with subwavelength resolution and Laplace filtering. Perhaps for more...

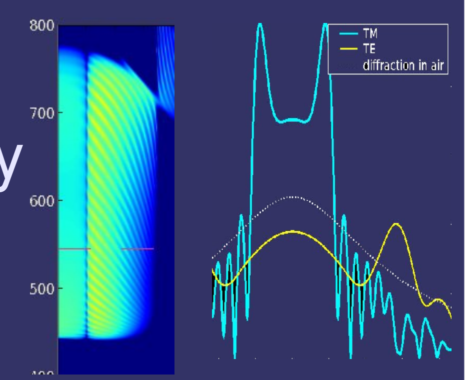

- A variety of transmission characteristics is possible: eg. for resonant tunnelling – one has a broadband widely tailored transparency spectral region, irregular shape of PSF, transparency at distances larger than wavelength.

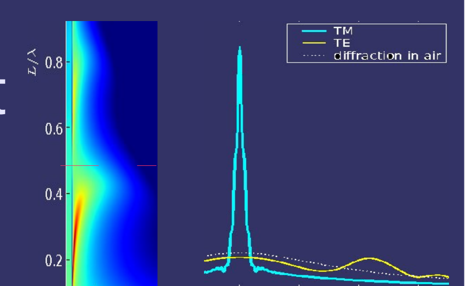

for canalization – regular PSF; transmission at resonant frequencies only; multilayer width is limited by losses

Acknowledgements

University of Warsaw

Prof. Tomasz Szoplik
dr. Jacek Pniewski
Tomsz Stefaniuk
Karol Król

Vrije Universiteit Brussel

Prof. Krassimir Panajotov

Projects/ frameworks

- Polish grant 0694/H03/2007/32

- COST actions MP 0702, MP0803